iScience

CellPress

Article

RECK in Neural Precursor Cells Plays a Critical Role in Mouse Forebrain Angiogenesis

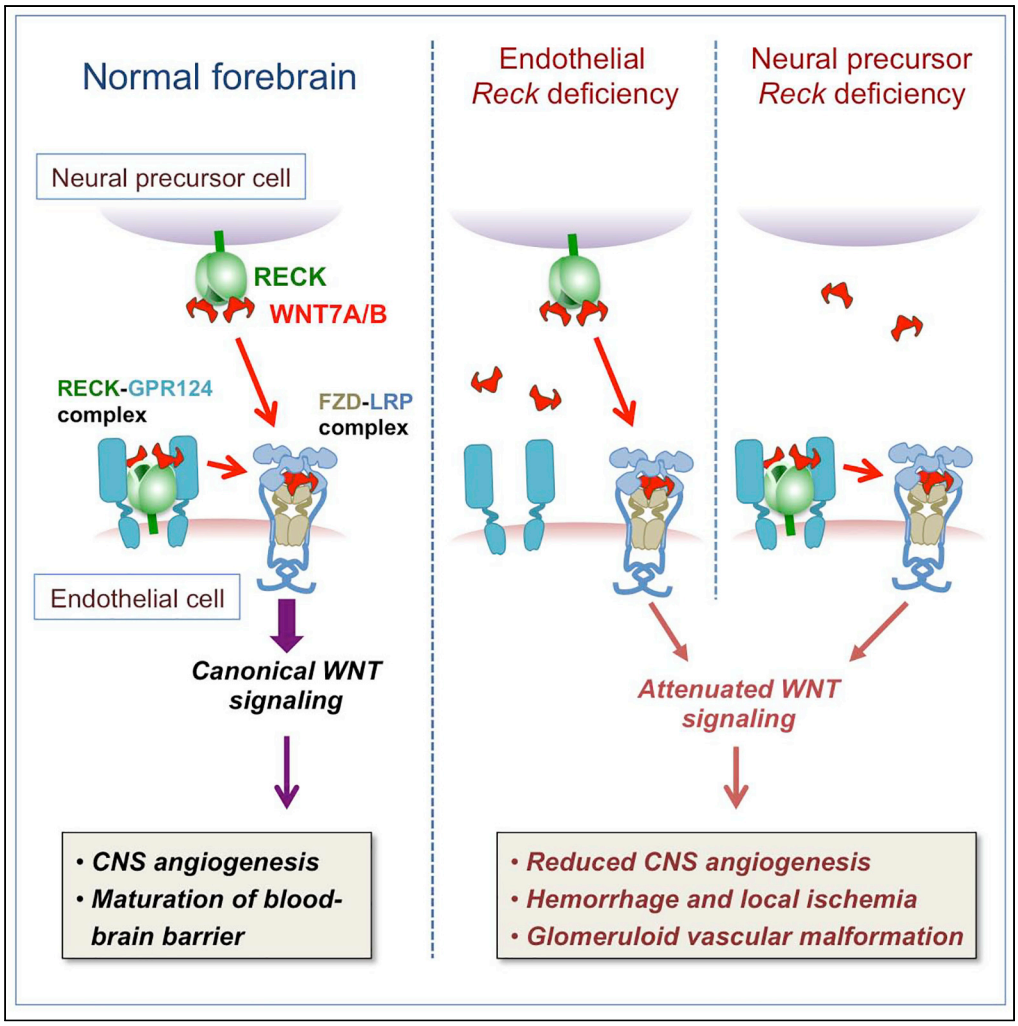

Huiping Li, Takao Miki, Glícia Maria de Almeida, ..., Calvin J. Kuo, Naoki Watanabe, Makoto Noda

noda.makoto.3x@kyoto-u.ac.jp

HIGHLIGHTS

Mice lacking RECK in *Foxg1*-positive neural precursor cells die shortly after birth

These mice show vascular defects similar to those in mice lacking endothelial RECK

The vascular phenotype can be suppressed by LiCl, an activator of WNT signaling

RECK in WNT7-producing cell enhances contact-dependent WNT signaling in adjacent cells

Li et al., iScience *19*, 559–571
September 27, 2019
https://doi.org/10.1016/j.isci.2019.08.009

iScience

CellPress

Article

RECK in Neural Precursor Cells Plays a Critical Role in Mouse Forebrain Angiogenesis

Huiping Li,[1,2] Takao Miki,[1] Glícia Maria de Almeida,[1] Carina Hanashima,[3] Tomoko Matsuzaki,[1] Calvin J. Kuo,[4] Naoki Watanabe,[2,5] and Makoto Noda[1,6,*]

SUMMARY

RECK in neural precursor cells (NPCs) was previously found to support Notch-dependent neurogenesis in mice. On the other hand, recent studies implicate RECK in endothelial cells (ECs) in WNT7-triggered canonical WNT signaling essential for brain angiogenesis. Here we report that RECK in NPCs is also critical for brain angiogenesis. When *Reck* is inactivated in *Foxg1*-positive NPCs, mice die shortly after birth with hemorrhage in the forebrain, with angiogenic sprouts stalling at the periphery and forming abnormal aggregates reminiscent of those in EC-selective *Reck* knockout mice and *Wnt7a/b*-deficient mice. The hemorrhage can be pharmacologically suppressed by lithium chloride. An effect of RECK in WNT7-producing cells to enhance canonical WNT-signaling in reporter cells is detectable in mixed culture but not with conditioned medium. Our findings suggest that NPC-expressed RECK has a non-cell-autonomous function to promote forebrain angiogenesis through contact-dependent enhancement of WNT signaling in ECs, implying possible involvement of RECK in neurovascular coupling.

INTRODUCTION

Precise bidirectional communications between the nervous and vascular systems (i.e., neurovascular coupling) is essential for proper formation and functioning of the central nervous system (CNS) in vertebrates (Paredes et al., 2018). Several neuroepithelium-derived molecules crucial for CNS-specific angiogenesis have been discovered, which include ID1/ID3 (Lyden et al., 1999), integrin alpha-V (Bader et al., 1998; McCarty et al., 2002, 2005), integrin beta-8 (Zhu et al., 2002; Proctor et al., 2005), WNT7A/B (Stenman et al., 2008; Daneman et al., 2009), and TGFBR2 (Hellbach et al., 2014). However, it remains to be elucidated exactly how these molecules contribute to the neurovascular communication.

RECK (reversion-inducing cysteine-rich protein with Kazal motifs) encodes a glycosylphosphatidylinositol-anchored glycoprotein capable of regulating several extracellular metalloproteinases (Takahashi et al., 1998). Global *Reck* knockout mice die around embryonic day 10.5 (E10.5) with reduced tissue integrity, abdominal hemorrhage (Oh et al., 2001), and precocious neuronal differentiation (Muraguchi et al., 2007). Around E10.5, normal mice express RECK abundantly in blood vessels (both endothelial cells [ECs] and mural cells) as well as neural precursor cells (NPCs) (Oh et al., 2001; Muraguchi et al., 2007; Chandana et al., 2010). To explore the functions of RECK in mice beyond E10.5, we generated *Reck*-flox mice (Chandana et al., 2010; Yamamoto et al., 2012). Our earlier study using temporally inducible *Reck* knockout mice revealed that inactivation of *Reck* at around E11 results in vascular defects including forebrain hemorrhage and vascular malformation by E15.5 and embryonic death before birth (Chandana et al., 2010). The roles of RECK in different cell types, however, could not be discriminated in such system. A more recent study using cell type-selective *Reck* knockout mice revealed that *Reck* inactivation in mural cells recapitulates the E10.5 lethality of global knockout mice, whereas *Reck* inactivation in ECs results in perinatal death with brain hemorrhage (Almeida et al., 2015), further highlighting the importance of RECK in vascular development.

Recent studies also indicate that RECK binds and cooperates with GPR124, an orphan G-protein-coupled receptor, to facilitate the canonical WNT signaling in ECs triggered by WNT7A/B that is required for proper tip cell function, CNS angiogenesis, and blood-brain barrier maturation (Vanhollebeke et al., 2015; Ulrich et al., 2016; Cho et al., 2017; Vallon et al., 2018). Interestingly, RECK was found to directly

[1]Department of Molecular Oncology, Kyoto University Graduate School of Medicine, Yoshida-Konoe-cho, Sakyo-ku, Kyoto 606-8501, Japan

[2]Laboratory of Single-Molecule Cell Biology, Kyoto University Graduate School of Biostudies, Yoshida-Konoe-cho, Sakyo-ku, Kyoto 606-8501, Japan

[3]Department of Biology, Faculty of Education and Integrated Arts and Sciences, Waseda University, Shinjuku-ku, Tokyo 162-8480, Japan

[4]Stanford University School of Medicine, Department of Medicine, Division of Hematology, Lokey Stem Cell Research Building, 265 Campus Drive, Stanford, CA 94305, USA

[5]Department of Pharmacology, Kyoto University Graduate School of Medicine, Yoshida-Konoe-cho, Sakyo-ku, Kyoto 606-8501, Japan

[6]Lead Contact

*Correspondence: noda.makoto.3x@kyoto-u.ac.jp

https://doi.org/10.1016/j.isci.2019.08.009

bind WNT7A/B and confer ligand specificity to the FZD4-LRP5/6 receptor complex (Eubelen et al., 2018; Vallon et al., 2018).

As our earlier study using global *Reck* knockout mice implicated RECK in CNS development (Muraguchi et al., 2007), we attempted to confirm and extend that finding by inactivating *Reck* selectively in the *Foxg1*-positive NPCs in mice, expecting to find some neural deficiency. Characterization of these mice, however, revealed an unexpected role for NPC-expressed RECK in CNS angiogenesis.

RESULTS

Reck Knockout in *Foxg1*-Positive NPCs Results in Neonatal Death with Unexpected Phenotype of Forebrain Hemorrhage

To selectively inactivate *Reck* in NPCs, we chose to use a *Foxg1-Cre* transgenic line (Hebert and McConnell, 2000). When visualized with the mTmG reporter system (Muzumdar et al., 2007), *Foxg1-Cre*-expressed cells (i.e., green cells in *mTmG;Foxg1-Cre* mice) are abundant in telencephalon at E8.5 and persist in a large area of the forebrain from E9.5 onward (Figure 1A; green signals). We generated mice carrying this *Foxg1-Cre* allele and one or two *Reck*-flox allele(s). The *Reck*-flox heterozygotes ($Reck^{flex1/+}$; *Foxg1-Cre*) are normal in gross morphology, fertile, and hence used as a control in this study. On the other hand, the *Reck*-flox homozygotes ($Reck^{flex1/flex1}$;*Foxg1-Cre*), which we call Reck-cKO (Foxg1), are not found among the adult littermates obtained from the mating supposed to yield such offspring at the 25% frequency (i.e., $Reck^{flex1/+}$;*Foxg1-Cre* x $Reck^{flex1/flex1}$). Careful examination of newborn pups revealed that Reck-cKO (Foxg1) mice are viable up to the day of birth (P0) but die shortly after birth exhibiting forebrain hemorrhage (Figure 1B). When traced back, visible forebrain hemorrhage occurred in 74% (29/39) of Reck-cKO (Foxg1) mice at E12.5 (Figure 1C, red diamond) and in all Reck-cKO (Foxg1) mice at E13.5 (Figure 1D, arrow) as well as at later embryonic time points (Figure 1C, E13.5–E18.5). Histological examinations indicate that hemorrhage mainly occurs in ganglionic eminence (GE) at early stages (Figure 1E-1, arrows) but becomes prominent in cerebral cortex (Cx) at later stages (Figure 1E-3, arrows). Immunofluorescence staining of brain sections of *mTmG;Foxg1-Cre* reporter mice, as shown in Figure 1A, indicates that *Foxg1-Cre*-expressed cells are neither CD31 positive (vascular ECs) nor NG2 positive (vascular mural cells) (Figure 1F). A previous study by Hellbach et al. also indicated that *Foxg1-Cre* is expressed in neuronal cells, but not in vascular cells, in the forebrain in this transgenic line (Hellbach et al., 2014). These data support the idea that the phenotype of Reck-cKO (Foxg1) mice results from the lack of RECK in NPCs rather than vascular cells.

Reck-cKO (Foxg1) Embryos Exhibit Vascular Malformations

CD31 is known to be expressed in ECs and some blood cells (Privratsky et al., 2010). When forebrain sections from E12.5 embryos were stained with anti-CD31, a line of regularly spaced small loops (representing cross sections of blood vessels) was found near the ventricular edge of both GE and Cx in control mice (Figures 2B and 2C, arrows). In Reck-cKO (Foxg1) mice, however, abnormal aggregates of CD31-positive cells or loops are found in GE near the perineural vascular plexus or midway toward the ventricle (Figure 2E, arrowheads); these abnormal vessels are proliferative (Figure S1A) and reminiscent of the glomeruloid malformations found in *Wnt7A/Wnt7b* double-knockout mice (Stenman et al., 2008; Daneman et al., 2009) and *Gpr124* knockout mice (Kuhnert et al., 2010). On the other hand, very few vessels were found in the cortex of Reck-cKO (Foxg1) mice (Figure 2F).

Less severe but similar vascular abnormalities were found in cKO (Foxg1) mice at E11.5 (Figures 2L–2P). In GE, CD31-positive (red) cells form multilayered tubes with wide opening that are associated with NG2-positive (green) cells (Figure 2O, arrowheads).

At E13.5, Reck-cKO (Foxg1) mice show more advanced vascular abnormalities, including the lack of a line of regularly spaced periventricular vessels (Figures 3G and 3H; see arrows in Figures 3C and 3D); large aggregates of CD31-positive, proliferative cells midway toward the ventricle (Figure 3G, arrowheads; Figures S1B–S1D); and a central region of apparent tissue damage (Figure 3G, asterisk) in GE. In the cortex, some vessels consisting of multilayered CD31-positive cells with round luminal space are found in the cortex (Figure 3H, arrowheads).

Taken together, these findings indicate that *Reck* expressed in NPCs is critical for proper angiogenesis in the forebrain, especially in GE and Cx.

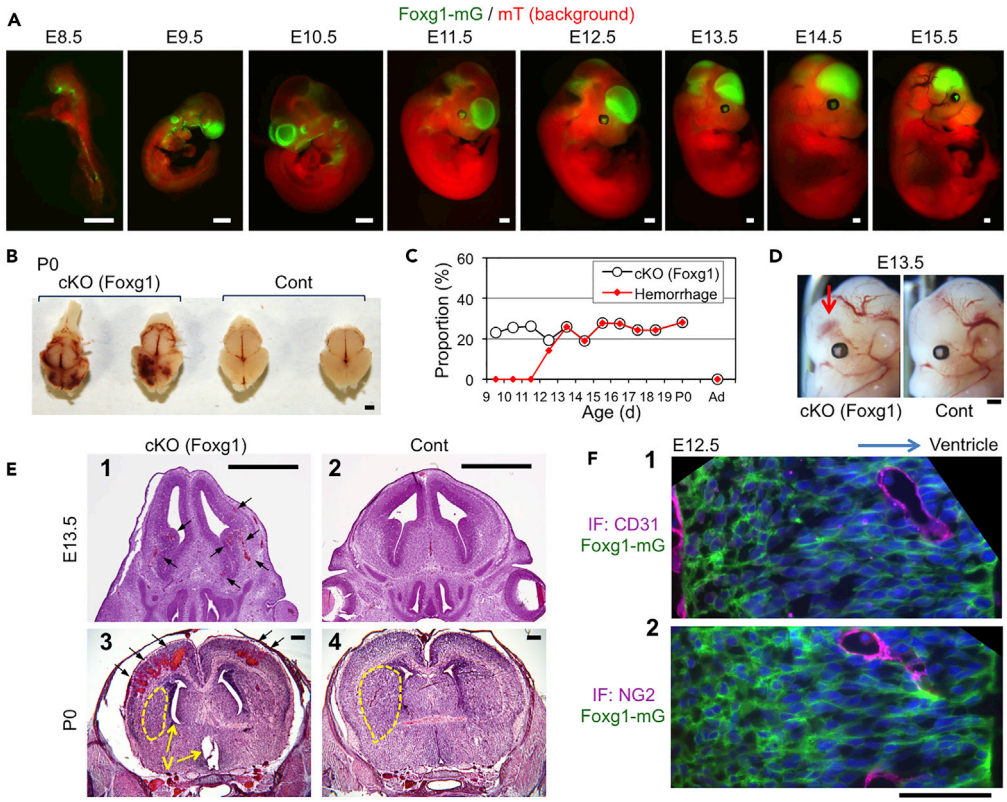

Figure 1. Selective Inactivation of *Reck* in *Foxg1*-Positive Cells (i.e., NPCs) in Mice Results in Cerebral Hemorrhage and Neonatal Death

(A) Expression of *Foxg1-Cre* in mouse embryo as visualized in *mTmG;Foxg1-Cre* mice. Green signals represent *Foxg1-Cre*-expressed cells.

(B) Typical dorsal views of the brains from Reck-cKO (Foxg1) mice (left two samples) and control mice (right two samples) at P0.

(C) Proportion of Reck-cKO (Foxg1) mice (open circle) and the mice with cerebral hemorrhage (red diamond) among the littermates ($n \geq 26$) at indicated stage obtained after mating between $Reck^{flex1/+}$;*Foxg1-Cre* mice and $Reck^{flex1/flex1}$ mice. Note that Reck-cKO (Foxg1) mice were found at the Mendelian ratio (~25%) from E9.5 to P0 but never among the adult mice. From E13.5 to P0, all Reck-cKO (Foxg1) mice exhibited cerebral hemorrhage.

(D) Lateral views, focusing on the head region, of Reck-cKO (Foxg1) (left) and control (right) embryos at E13.5. The typical red spot (arrow) above the eye, commonly found in Reck-cKO (Foxg1) embryos, corresponds to hemorrhage in GE.

(E) H&E-stained coronal sections of the brains from Reck-cKO (Foxg1) mice (panels 1 and 3) or control mice (panels 2 and 4) at E13.5 (panels 1 and 2) or P0 (panels 3 and 4). Note the numerous microscopic hemorrhage in the Reck-cKO (Foxg1) mouse brains at both stages (arrows in panels 1 and 3) and larger ventricles (V) and smaller striatum (the area indicated by dotted line) in the Reck-cKO (Foxg1) mouse at P0 (compare panel 3 with panel 4).

(F) Coronal sections of *mTmG;Foxg1-Cre* mice (as used in A) at E12.5 were immunostained (magenta) with antibodies against CD31 (EC marker, panel 1) or NG2 (mural cell marker, panel 2) followed by nuclear counterstain (blue). Note that magenta signals (vascular cells) and green signals (Foxg1-expressed cells) are essentially non-overlapped.

Scale bars: 500 μm in (A), 1 mm in (B, D, and E), and 50 μm in (F).

Reck-cKO (Foxg1) Embryos Exhibit Precocious Neuronal Differentiation

The vascular abnormalities in the forebrains of Reck-cKO (Foxg1) mice are accompanied by the increased number and widened zone of TUJ1-positive differentiated neurons (Figure 2Q, compare green signals in panels 1 and 2) and the reduced number and narrower zone of Ki67-positive proliferative cells in both Cx and GE (Figure S2). Hence, precocious neuronal differentiation, a phenotype previously found in global *Reck* knockout mice (Muraguchi et al., 2007), is recapitulated in Reck-cKO (Foxg1) mice, suggesting that RECK produced by NPCs affects both neurogenesis and angiogenesis.

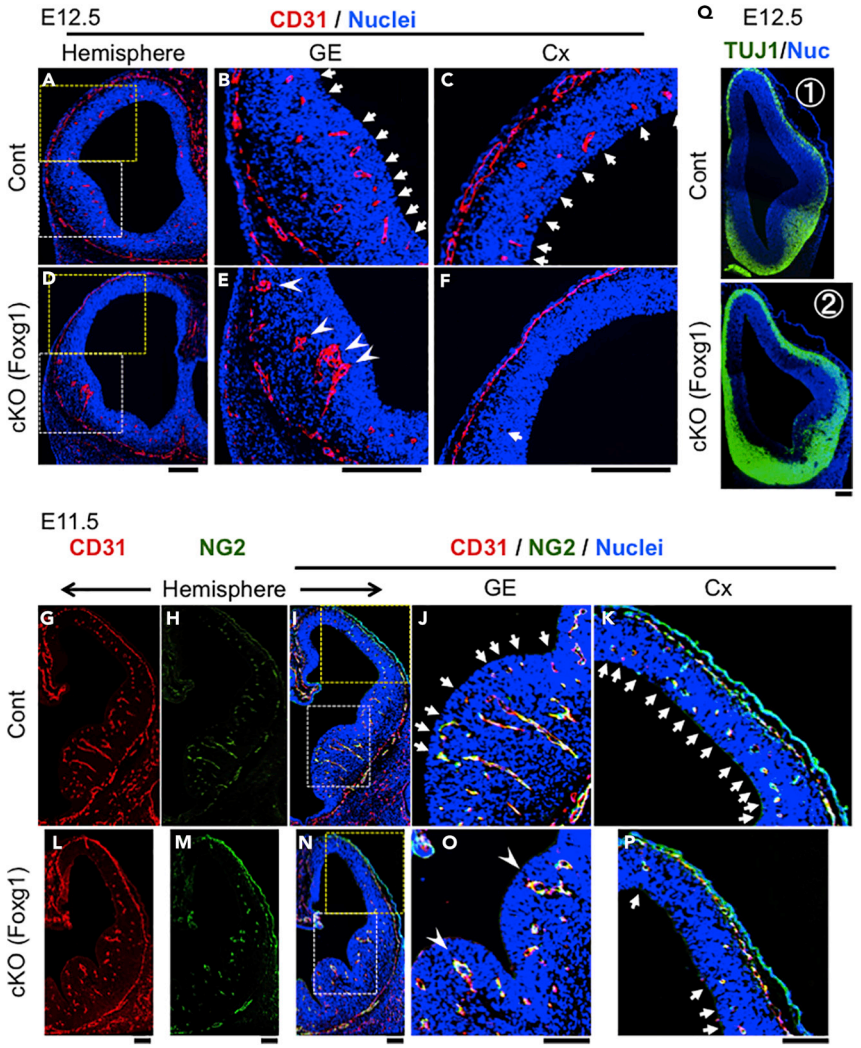

Figure 2. Vascular and Neuronal Phenotypes of Mice Lacking *Reck* Expression in NPCs

(A–F) Vascular phenotype of Reck-cKO (Foxg1) mouse at E12.5. A coronal section of the brain from control (A–C) or Reck-cKO (Foxg1) mouse (D–F) at E12.5 was stained with anti-CD31 antibodies (red) followed by nuclear counterstain (blue). Magnified views of the two areas (dotted-line box) in (A and D) are shown in (B) GE and (C) cortex and (E) GE and (F) cortex, respectively. Note that typical glomeruloid malformations are found in the GE of Reck-cKO (Foxg1) mouse (arrowheads in E) and that a line of regularly spaced small vessels along the ventricular edge in the control mouse (arrows in B and C) are absent in Reck-cKO (Foxg1) mouse (E and F).

(G–P) Vascular phenotype of Reck-cKO (Foxg1) mouse at E11.5. A coronal section of the brain from control (G–K) or Reck-cKO (Foxg1) mouse (L–P) at E11.5 was double stained with antibodies against CD31 (red) and NG2 (green) followed by nuclear counterstain (blue). Single-color images for CD31 (G and L) and NG2 (H and M) as well as three-color images (I–K and N–P) are shown. Magnified views of the two areas (dotted-line box) in (I and N) are shown in (J) GE and (K) cortex and (O) GE and P cortex, respectively. Note the abnormal vessels in GE (O) and that a line of regularly spaced small vessels, as found in the control mouse (arrows in J and K), is absent in Reck-cKO (Foxg1) mouse (O and P).

(Q) Neural phenotype of Reck-cKO (Foxg1) mouse at E12.5. A coronal section of the brain from control mouse (panel 1) or Reck-cKO (Foxg1) mouse (panel 2) at E12.5 was stained with anti-TUJ1 antibodies (green) followed by nuclear counterstain (blue). Note the expanded TUJ1-positive area in the Reck-cKO (Foxg1) mouse brain (panel 2). Scale bars, 200 μm.

See also Figures S1–S3.

Reck Deficiency in NPC and *Reck* Deficiency in EC Lead to Similar Vascular Phenotype

For comparison, we generated EC-selective conditional knockout mice using a Tie2-Cre transgenic line (Kisanuki et al., 2001). The *Reck*$^{flex1/flex1}$;*Tie2-Cre* mice (Reck-cKO [Tie2] mice in short) show phenotypes

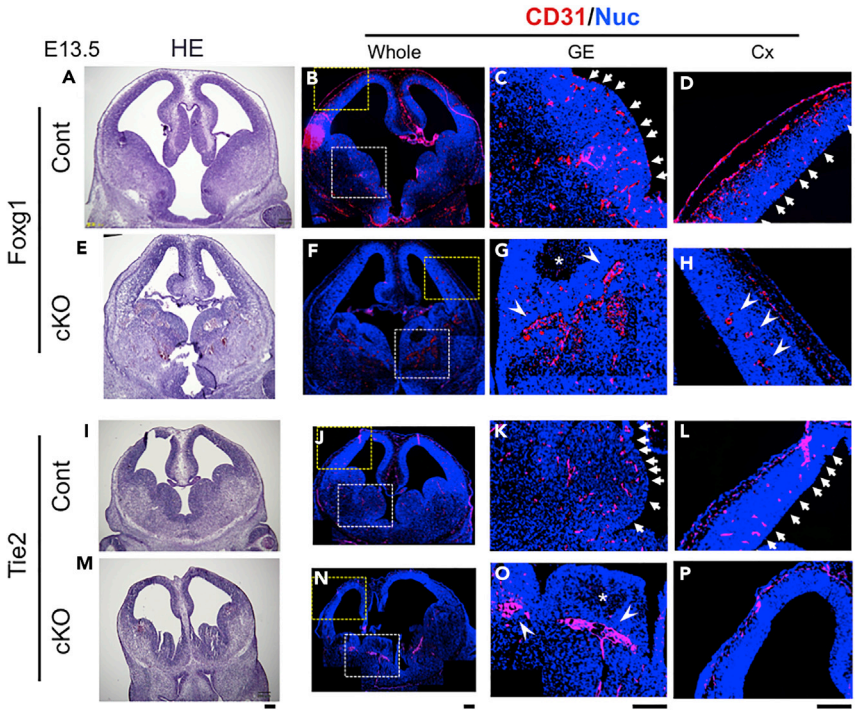

Figure 3. Effects of *Reck* Mutations in NPCs and ECs

(A–H) (A–E) Vascular phenotype of Reck-cKO (Foxg1) mice at E13.5. Serial coronal sections of the brain from control (A–D) or Reck-cKO (Foxg1) mouse (E–H) at E13.5 were prepared, and one section was H&E-stained (panels A and E) and the next section was fluorescently stained with anti-CD31 antibodies (red) followed by nuclear counterstain (blue) (B–D and F–H). Magnified views of the two areas (dotted-line box) in (B and F) are shown in (C) GE and (D) cortex and (G) GE and (H) cortex, respectively. Note that large glomeruloid malformations are found in the GE of Reck-cKO (Foxg1) mouse (arrowheads in G) and that a line of regularly spaced small vessels along the ventricular edge in the control mouse (arrows in C and D) is absent in Reck-cKO (Foxg1) mouse (G and E). Instead, a few larger and irregularly located vessels are found in the cortex of mutant mice (arrowheads, H).

(I–P) Vascular phenotype of Reck-cKO (Tie2) mice at E13.5. Serial coronal sections of the brain from control (I–L) or Reck-cKO (Tie2) mouse (M–P) at E13.5 were prepared, stained, and presented as described for (A–H). Note the phenotype very similar to that of Reck-cKO (Foxg1) mice, including large glomeruloid malformations in GE (arrowheads in O) and the absence of regularly spaced small vessels along the ventricular edge (compare O and P with K and L). Scale bars, 200 μm. See also Figures S1 and S3.

reminiscent of those of Reck-cKO (Foxg1) mice. For instance, at E13.5, the lack of a line of regularly spaced periventricular vessels in both the GE and cortex (Figures 3O and 3P; see arrows in Figures 3K and 3L), large aggregates of CD31-positive cells (Figure 3O, arrowheads), and a central tissue damage (Figure 3O, asterisk) in GE are evident. On the other hand, misexpression of TUJ1 is not observed in Reck-cKO (Tie2) mice (Figure S3), suggesting distinct effects of *Reck* in ECs and NPCs (see Figures 2Q and S2) on neuronal differentiation. Nevertheless, our data indicate that *Reck* deficiency in ECs and *Reck* deficiency in NPCs give rise to a vascular phenotype very similar both in timing and locations in the forebrain.

Vascular Phenotype of Reck-cKO (Foxg1) Mice Can Be Partially Rescued by Pharmacological Treatment with LiCl

Importance of the WNT7a/WNT7b-dependent canonical WNT signaling in brain angiogenesis (Stenman et al., 2008; Daneman et al., 2009) and the EC-autonomous function of RECK to specifically enhance such signaling (Vanhollebeke et al., 2015; Ulrich et al., 2016; Cho et al., 2017; Eubelen et al., 2018; Vallon et al., 2018) has been demonstrated. However, because RECK is a membrane-anchored protein, it is not obvious how the RECK expressed in NPCs can also affect angiogenesis. To address this question, we first tested whether canonical WNT signaling is affected in Reck-cKO (Foxg1) mice by daily administration of lithium chloride (LiCl) into the pregnant mice followed by morphological examination of Reck-cKO (Foxg1) embryos. LiCl is known to inhibit glycogen synthase kinase-3β thereby bypassing the

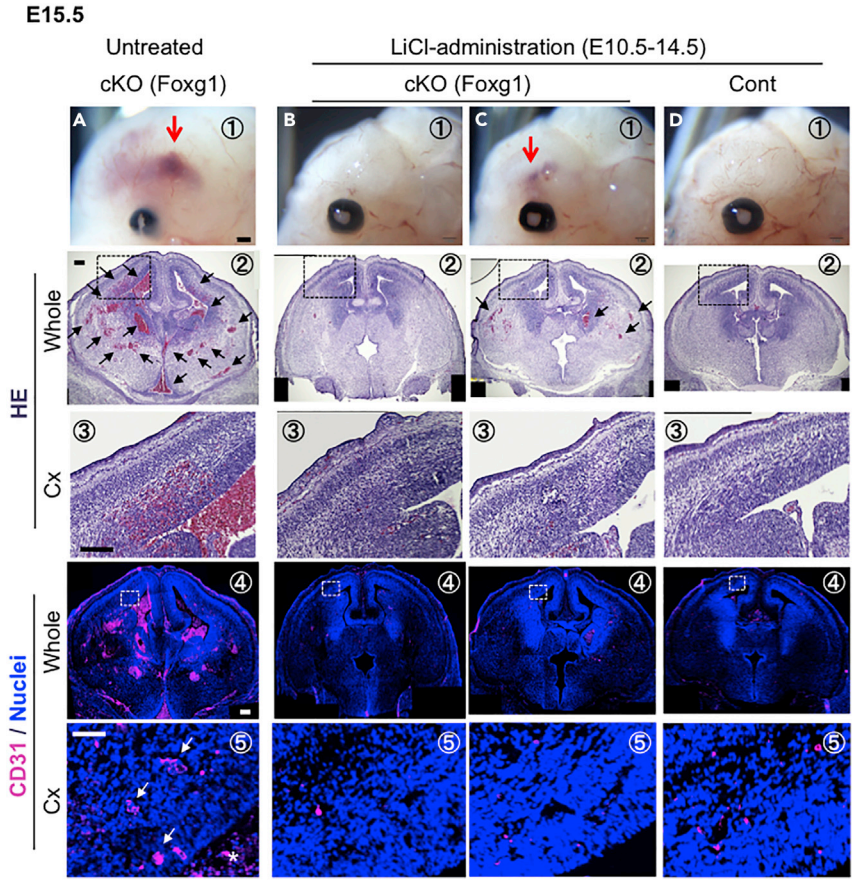

Figure 4. Effects of LiCl on the Vascular Phenotype of Reck-cKO (Foxg1) Mice

(A) Vascular phenotype of Reck-cKO (Foxg1) mice at E15.5 (untreated control). Panel 1: Lateral view of an intact, typical mutant embryo exhibiting cerebral hemorrhage (red arrow). Panel 2: an H&E-stained coronal section with numerous hemorrhagic legions (black arrows). Panel 3: magnified view of the cortical area shown by dotted-line box in panel 2. Panel 4: the next section subjected to immunofluorescence staining with anti-CD31 antibodies (red, vascular endothelial cells and some blood cells) followed by nuclear counterstain (blue). Panel 5: magnified view of a cortical area indicated by dotted-line box in panel 4.

(B and C) Two Reck-cKO (Foxg1) embryos harvested at E15.5 from pregnant mice pretreated with daily injection of LiCl from E10.5 to E14.5. Images in panels 1–5 were similarly acquired as those in (A). Note that hemorrhagic legions are greatly reduced in number and size in one case (C) and almost absent in the other case (B).

(D) Control embryos harvested at E15.5 from pregnant mice pretreated with daily injection of LiCl from E10.5 to E14.5 (LiCl-treated control mouse). Scale bars, 200 μm.

See also Figure S4.

ligand-receptor interactions and directly activating downstream cascade of canonical WNT signaling (Klein and Melton, 1996); the agent has been used to demonstrate the involvement of canonical WNT signaling during various developmental processes in mouse embryos (Cohen et al., 2007, 2009; Kugimiya et al., 2007; Tian et al., 2010; Griffin et al., 2011; Curtis and Griffin, 2012; Cornett et al., 2013; Cambier et al., 2014; Briggs et al., 2015; Da Silva et al., 2017).

First, untreated Reck-cKO (Foxg1) mice at E15.5 show hemorrhage in both GE and the cortex (Cx) at 100% penetrance (Figure 4A; Table 1, a; Figure S4). In contrast, daily administration of LiCl from E8.5 to E14.5 suppressed macroscopic hemorrhage completely in the cortex and partially in GE (Table 1, b). We therefore compared the effects of LiCl injected at different timings. The results indicate that the treatments from E10.5 to E14.5 (Table 1, d) are essential for this suppression. Histological examinations of the LiCl-treated mice indicated that small hemorrhagic legions were found in GE in some of the animals but not in their cortices (Figures 4B and 4C); this was in sharp contrast to the numerous large hemorrhagic legions found

Schedule for Daily Administration of LiCl (200 mg/kg/day, i.p.)								Number of Embryos [(Hemorrhage at E15.5)/ (cKO Embryos Examined)]	
Stage (E)	8.5	9.5	10.5	11.5	12.5	13.5	14.5	Ganglionic Eminence	Cerebral Cortex
a								45/45	45/45
b	×	×	×	×	×	×	×	3/4	0/4
c	×	×	×	×	×			2/2	2/2
d			×	×	×	×	×	9/11	0/11
e				×	×	×	×	5/5	1/5
f					×	×		3/3	3/3

Table 1. Suppression of Forebrain Hemorrhage by LiCl-Administration
i.p., intraperitoneal injection; cKO, conditional knockout (Reckflex1/flex1;Foxg1-Cre); x, LiCl injected. See also Figure S4.

in both the GE and the cortex of untreated animals that resulted in the leakage of blood into the ventricles (Figure 4A). These findings support the idea that RECK in NPCs influences canonical WNT signaling.

Altered Gene Expression Is Found in the Embryonic Forebrain of Reck-cKO (Foxg1) Mouse

To gain some insights into the possible mechanism by which RECK in NPCs may affect canonical WNT signaling and vascular development in the forebrain, we determined the levels of mRNAs encoding some molecules relevant to brain development, angiogenesis, and WNT signaling using total RNA extracted from forebrain of embryos at three time points (E11.5, E12.5, and E13.5) by quantitative reverse-transcriptase polymerase chain reaction (qRT-PCR) (Figure 5A). At the first time point (E11.5; blue symbols), significant downregulation of an NPC marker, *Nes*, was detected (Figure 5A, group 23). At the second time point (E12.5; red symbols), upregulation of *Mmp2* (protease), *Id3* (transcription factor), and downregulation of *Wnt7a*, *Itg8b* (cell adhesion receptor), and two endogenous targets of canonical WNT signaling, *Apcdd1* and *Sox17*, became significant (Figure 5A, groups 3, 6, 12, 38, and 41). At the third time point (E13.5; green symbols), significant upregulation of *Mmp2*, *Vegfa* (vascular endothelial growth factor A), downregulation of *Wnt7a*, *Wnt7b*, *Apcdd1*, *and Sox17* were noted (Figure 5A, groups 4, 7, 10, 22, 39, and 42). Downregulation of *Apcdd1* and *Sox17* provides additional evidence suggesting that canonical WNT signaling is affected by the *Reck* deficiency. Some of the other alterations in gene expression may directly or indirectly contribute to the mutant phenotype (see Discussion).

RECK in NPCs or Ligand-Producing Cells Can Enhance Contact-Dependent Activation of Canonical WNT Signaling in Reporter Cells

Neuroepithelium-derived WNT7A/B (leading to canonical Wnt signaling in CNS ECs) is known to be specifically required for CNS vascularization (Stenman et al., 2008; Daneman et al., 2009). To test whether RECK in NPCs may enhance canonical WNT signaling in a non-cell-autonomous fashion, we prepared NPCs from Reck-cKO (Foxg1) mice and control mice at E11.5. These NPCs (Figures 5B and 5C, groups 1 and 2; Figure S5, group 11) or their conditioned media (Figure 5C, groups 3 and 4) were overlaid onto the TOP-Flash reporter cells expressing FZD4, LRP5, GPR124, and RECK, and the cultures were incubated for 24 h followed by luciferase assay to detect canonical WNT signaling. NPCs stimulated WNT signaling when mixed with the reporter cells (Figure S5, groups 9 versus 11; Figures 5B and 5C, group 1), but their conditioned media failed to do so (Figure 5C, group 3), indicating contact-dependent stimulation. Furthermore, NPCs prepared from Reck-cKO (Foxg1) mice were less effective than the control NPCs in this assay (Figures 5B and 5C, groups 2 versus 1). These results suggest that NPCs display ligand(s) (on their surface) stimulating canonical WNT signaling in adjacent reporter cells and that RECK somehow enhances this stimulation.

We also performed a model experiment using HEK293 cells in which the effects of RECK in both ligand-producing cells and TOP-Flash reporter cells were assessed. To prepare the assay system, we first established a series of derivatives of RECK-deficient HEK293 cells producing WNT7A or WNT7B (Producers) or

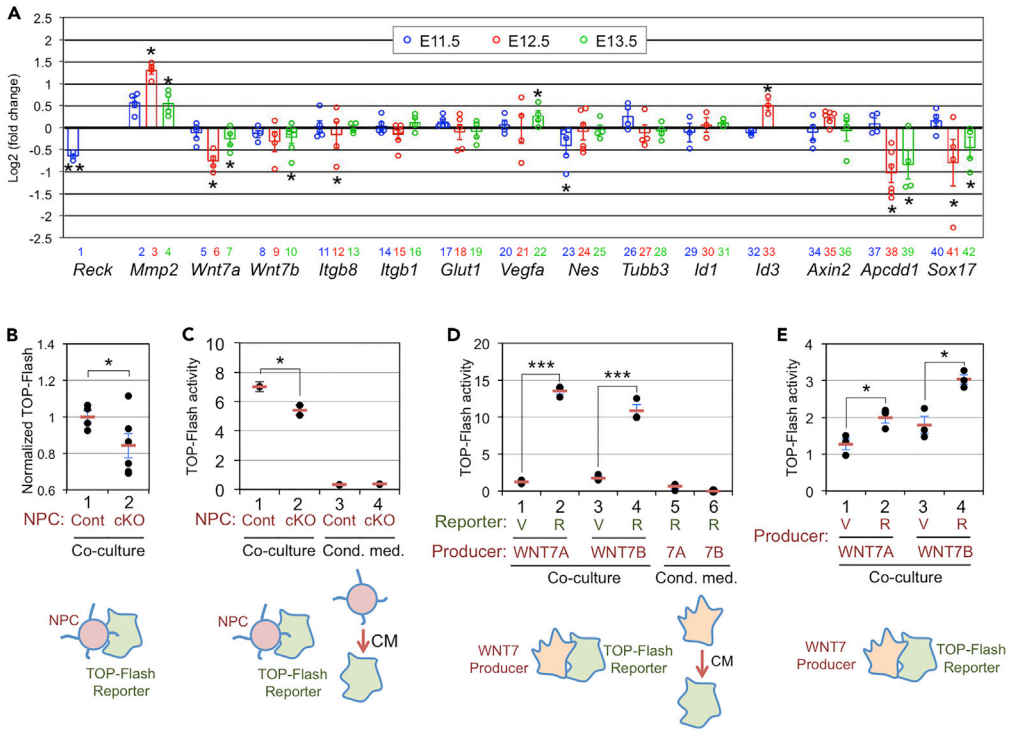

Figure 5. The Effects of RECK on Gene Expression in the Forebrain and Canonical WNT Signaling in Adjacent Cells

(A) Changes in the levels of mRNAs encoding 15 proteins considered to be relevant to the vascular or neural phenotypes of Reck-cKO (Foxg1) mice and WNT/β-catenin signaling. Total RNA extracted from the forebrains of control mice and Reck-cKO (Foxg1) mice at E11.5, E12.5, and E13.5 were subjected to qRT-PCR using primer sets specifically amplifying indicated mRNAs and internal control (*Gapdh* or *Mars*). The level of mRNA relative to the control in each sample was calculated, and then the ratio of the values for Reck-cKO (Foxg1) mice and control mice is presented in dot plots with open bar representing mean ± SEM. Vertical axis is in the $\log_2$ scale. *$p < 0.05$, **$p < 0.01$.

(B) The ability of NPCs to activate canonical WNT signaling in the reporter cells in mixed culture. NPCs prepared from the forebrains of control embryos (n = 4, group 1) or Reck-cKO (Foxg1) embryos (n = 6, group 2) were co-cultured for 24 h with TOP-Flash reporter cells followed by dual-luciferase assay. Horizontal lines in each group represent mean (brown) and SEM (blue). *$p < 0.05$. Note that NPCs from Reck-cKO (Foxg1) mice show significantly lower activity to stimulate WNT signaling in the Reporter cells (group 2).

(C) The ability of NPCs and their conditioned media to activate canonical WNT signaling in the reporter cells. NPCs (groups 1 and 2) and their conditioned media (groups 3 and 4) were subjected to TOP-Flash assay as described in (B). Note that the activity of conditioned media (groups 3 and 4) were very low in this assay, indicating that the activity of NPCs to stimulate canonical WNT signaling in the reporter cells is contact dependent.

(D) The effect of RECK in the reporter cells on, and contact-dependence of, the WNT7-triggered canonical WNT signaling. HEK293 cells producing WNT7A (groups 1 and 2) or WNT7B (groups 3 and 4) or their conditioned media (groups 5 and 6) were added to the RECK-deficient TOP-Flash reporter cells transfected with either vacant vector (groups 1 and 3) or RECK expression vector (groups 2 and 4–6). After 24-h incubation, dual luciferase assay was performed. ***$p < 0.003$. Note that RECK in the reporter cells greatly enhances WNT signaling in this co-culture assay (groups 2 and 4) and that the stimulation could not be achieved with conditioned media (groups 5 and 6), demonstrating a cell-autonomous effect of RECK to enhance the contact-dependent, WNT7-stimulated WNT signaling.

(E) The effect of RECK in WNT7-producing HEK293 cells to stimulate WNT signaling in the reporter cells in mixed culture. RECK-deficient HEK293 cells stably expressing WNT7A (groups 1 and 2) or WNT7B (groups 3 and 4) were transfected with either control vector (V) or RECK expression vector (R), incubated for 48 h, and then co-cultured for 24 h with TOP-Flash reporter cells lacking RECK, followed by dual-luciferase assay (in triplicate). *$p < 0.05$. Note that RECK in WNT7-producing cells has the ability to enhance (1.6–1.7 fold) WNT signaling in the *RECK*-null reporter cells (i.e., non-cell-autonomous effect). Experiments were repeated three times with similar results.

See also Figure S5.

harboring the TOP-Flash reporter plasmid (Reporter). The Producer cells were then transfected with either a vacant vector (V) or RECK expression vector (R); the Reporter cells were transfected with expression vectors encoding the WNT7 receptor components: FZD4, LRP5, GPR124, and RECK (R) (or control vector [V]).

The Reporter cells were mixed and incubated with either the Producer cells or their conditioned media for 24 h and then subjected to the luciferase assay to assess WNT signaling. First, condition media from the Producer cells failed to induce robust WNT signaling even when RECK was expressed in the Reporter cells (Figure 5D, groups 5 and 6). When Producer cells were mixed and incubated with Reporter cells, robust WNT signaling was induced only when RECK was expressed in the Reporter cells (Figure 5D, groups 2 and 4), and hence the Reporter cell-autonomous effect of RECK to enhance contact-dependent stimulation of WNT signaling could be demonstrated in this system. When RECK was absent in the Reporter cells, RECK in Producer cells significantly increased the WNT signaling in the Reporter cells (Figure 5E, groups 2 and 4), demonstrating the non-cell-autonomous effect of RECK in ligand-producing cells to enhance the contact-dependent stimulation of WNT signaling in the adjacent Reporter cells. On the other hand, GPR124 in Producer cells does not cooperate with RECK in enhancing WNT signaling (Figure S5, groups 4 and 8).

DISCUSSION

Our previous study indicated that RECK in ECs is required for proper vascular development in mouse CNS (Almeida et al., 2015). It was also demonstrated that RECK facilitates the WNT7A/B-mediated canonical WNT-β-catenin signaling in ECs (Cho et al., 2017; Eubelen et al., 2018; Ulrich et al., 2016; Vallon et al., 2018; Vanhollebeke et al., 2015) that is required for CNS angiogenesis (Liebner et al., 2008; Stenman et al., 2008; Daneman et al., 2009). Our findings reported here indicate that RECK in neuroepithelial cells is also required for proper angiogenesis in the forebrain. Several lines of evidence, including (1) phenotypic resemblance among Reck-cKO (Foxg1) mice (Figures 1, 2, and 3), *Wnt7a/Wnt7b* double-knockout mice, and EC-specific β-catenin knockout mice (Liebner et al., 2008; Stenman et al., 2008; Daneman et al., 2009); (2) the effect of LiCl to suppress the vascular phenotype of Reck-cKO (Foxg1) mice (Figure 4); (3) reduced expression of *Apcdd1* and *Sox17* in the mutant forebrain (Figure 5A); and (4) the TOP-Flash data in mixed culture (Figures 5B–5E), point to the model that RECK in NPCs somehow facilitates contact-dependent, WNT7A/B-stimulated WNT-β-catenin signaling in ECs.

How could RECK in NPCs exert such non-cell-autonomous effects on WNT signaling in ECs? Recent studies have revealed the ability of RECK to specifically bind WNT7A/B, to keep them in a bioactive form (i.e., hydrophobic monomer) (Vallon et al., 2018), and to confer ligand specificity to the classical FZD-LRP5/6 receptor complex (Eubelen et al., 2018). One feasible model is that RECK expressed by WNT7-producing cells may help presenting bioactive ligands on their surface, thereby facilitating the contact-dependent cell-cell communication via these short-range ligands (Figure 6). We also speculate that the divalent nature of RECK dimer (Omura et al., 2009) may facilitate this task further, for instance, by promoting signalosome assembly. Such mechanism may also provide a solution to the "hand-over problem" in the intercellular WNT transport (Routledge and Scholpp, 2019).

Our gene expression data indicate upregulation of *Mmp2* in the forebrains of Reck-cKO (Foxg1) embryos (Figure 5A, groups 3 and 4). Although the relevance of this phenomenon to the mutant phenotype is unclear, upregulation of *Mmp2* mRNA was also observed in *Gpr124* knockout mice (Cullen et al., 2011). Downregulation of the NPC marker *Nes* at E11.5 (Figure 5A, group 23) may reflect the precocious neuronal differentiation (Figures 2Q-2 and S2), and yet upregulation of *Tubb3/Tuj1* was not so prominent. With regard to the neuronal differentiation, the ID family is also of interest, because *Id1/Id3* double-knockout mice die by E13.5 with brain hemorrhage and precocious neuronal differentiation (Lyden et al., 1999), which is similar in nature to, but different in timing of death from, the *Reck* mutant mice (Oh et al., 2001; Muraguchi et al., 2007; Chandana et al., 2010; Almeida et al., 2015). However, it is unclear whether the observed upregulation (rather than downregulation) of *Id3* at E12.5 (Figure 5A, group 33) contributes to the phenotype of Reck-cKO (Foxg1) mice.

Decreased expression of *Apcdd1* and *Sox17* (Figure 5A, groups 37–42) are indicative of attenuated WNT/β-catenin signaling in the forebrain of Reck-cKO (Foxg1) mice. As the products of these WNT-inducible genes are known to inhibit WNT/β-catenin signaling, their roles as negative feedback regulators have been postulated. Known properties and biological functions of these proteins, however, are intriguing in the present context. For instance, APCDD1 is a membrane-bound, cysteine-rich glycoprotein expressed in multiple tissues (including the nervous and vascular system as well as mesenchyme of several developing organs); it interacts with WNT3A and LRP5 and possibly prevents WNT-FZD binding (Shimomura et al., 2010; Cruciat and Niehrs, 2012). Hence, APCDD1 shares many similarities with RECK except that it inhibits

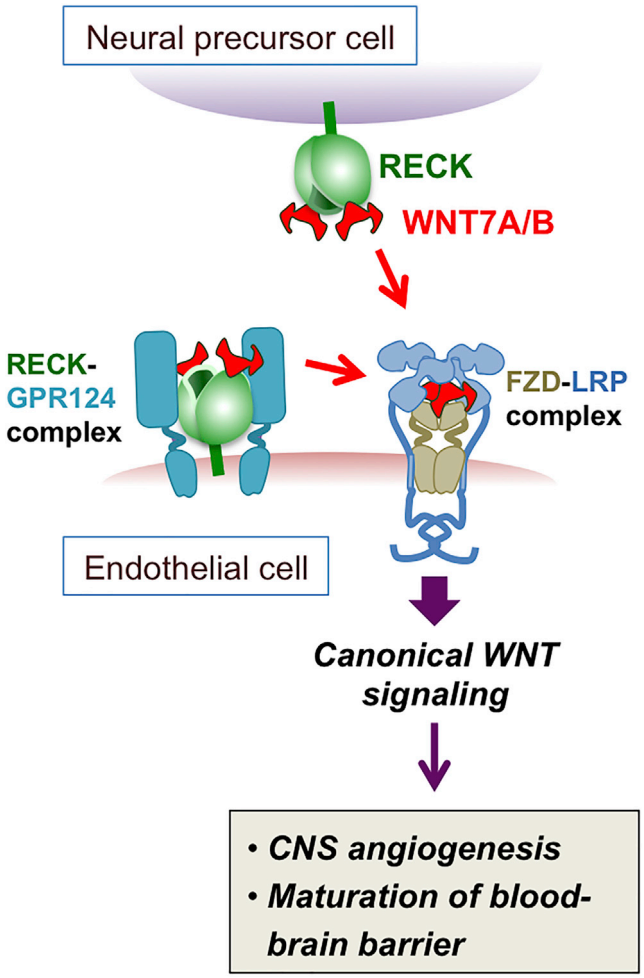

Figure 6. A Hypothetical Model to Explain How RECK on WNT7-Producing Cells (e.g., NPC) Could Enhance Contact-Dependent WNT7 Signaling in Adjacent Cells (e.g., Endothelial Cell)

The WNT7 receptor complex contains RECK, GPR124, FZD4, and LRP5; the direct interaction between WNT7 and RECK has been demonstrated (Eubelen et al., 2018; Vallon et al., 2018). As RECK is glycosylphosphatidylinositol anchored and forms cowbell-shaped dimer (Omura et al., 2009), it may serve as a divalent docking site for WNT7A/B on the cell surface. This model proposes that RECK might work in this way on both ligand-producing (upper side) and signal-receiving (lower side) cells, and the latter facilitates ligand transfer from one cell to the other. Ligand transfer may also be facilitated by some other, more indirect mechanisms, such as protection of WNT7A/B from proteolysis and stabilization of cell adhesion molecules to bring the cell surfaces of two cells closer to each other. Note that the 3D structures of RECK and GPR124 have not been solved so that the exact configuration among RECK, GPR124, and WNT7A/B is tentative. The configuration of dimeric WNT-FDZ-LRP complex is based on the crystal structure of the Wnt3a-Fzd8-Lrp6 complex recently reported by Takagi's group (Hirai et al., 2019).

(rather than promotes) Wnt/β-catenin signaling. Importantly, APCDD1 was found to coordinate vascular remodeling and barrier maturation of retinal blood vessels (Mazzoni et al., 2017). On the other hand, SOX17 is a transcription factor that forms a complex with β-catenin and several TCF/LEF family transcription factors and promotes their degradation (Zorn et al., 1999; Sinner et al., 2007). Of note, Sox17 bridges WNT and NOTCH signaling to promote arterial specification (Corada et al., 2013; Morini and Dejana, 2014) and blood-brain barrier maturation (Corada et al., 2019). Contribution of the reduction of these proteins to the vascular and/or neural phenotype of Reck-cKO (Foxg1) mice is an interesting possibility to be tested in future studies.

Wnt7a, *Wnt7b*, and *Itgb8* are known to be critical for CNS angiogenesis (Zhu et al., 2002; Proctor et al., 2005; Stenman et al., 2008; Daneman et al., 2009). Their downregulation from E12.5 or E13.5 in Reck-cKO

(Foxg1) mice (Figure 5A, groups 6, 7, 10, and 12) may also contribute to the progression of vascular phenotype in these mice, although the mechanisms by which these genes get downregulated remain unclear. The *Vegfa* upregulation found at E13.5 could be a consequence of hypoxia due to the halted vascularization, especially in the bulky tissues such as GE. The tissue damage at the center of GE (Figure 3G, asterisk) seems to support this idea. As vascular endothelial growth factor overexpression has been implicated in glomeruloid malformation (Sundberg et al., 2001) and intracranial hemorrhage (Yang et al., 2013), *Vegfa* upregulation may also contribute to the progressive nature of vascular defects in these mice.

In summary, we found that RECK on both endothelial and neuroepithelial components is essential for proper forebrain angiogenesis in mice. Our findings raise an interesting possibility that RECK mediates neurovascular communication by facilitating contact-dependent WNT signaling triggered by the short-range ligands WNT7A/B.

Limitations of the Study

Although our qRT-PCR experiments for *Apcdd1* and *Sox17* indicated attenuated WNT/β-catenin signaling in the forebrain of Reck-cKO (Foxg1) mice, it was not determined in which cell type(s) this attenuation occurs. We may address this issue more directly by cell-type-specific activation of canonical WNT signaling, for instance, using a dominant stable mutant of β-catenin (Harada et al., 1999). Our TOP-Flash assay *in vitro* supported the model that RECK in WNT7A/B-producing cells enhances contact-dependent activation of canonical WNT signaling in adjacent cells. However, the detailed molecular mechanism of this enhancement and whether such mechanism may account for all the vascular phenotype of Reck-cKO (Foxg1) mice remain to be elucidated. Previous studies indicate that WNT7A stimulates neuronal differentiation during brain development (Hirabayashi et al., 2004), that RECK promotes neurogenesis (NPC proliferation) by inhibiting Notch-ligand shedding (Muraguchi et al., 2007), and that GPR124 is not expressed in NPCs (Kuhnert et al., 2010; Anderson et al., 2011; Cullen et al., 2011). Whether RECK supports WNT7 signaling in NPCs (in the absence of GPR124) and whether defects in this mechanism contribute to the neural phenotype of Reck-cKO (Foxg1) mice remain to be addressed in future studies.

METHODS

All methods can be found in the accompanying Transparent Methods supplemental file.

SUPPLEMENTAL INFORMATION

Supplemental Information can be found online at https://doi.org/10.1016/j.isci.2019.08.009.

ACKNOWLEDGMENTS

This work was supported by KAKENHI to M.N. (Grants-in-Aid for Creative Scientific Research, Scientific Research on Priority Areas, and Scientific Research on Innovative Areas) and NIH grant to C.J.K. (NIH NS100904). H.L. was a MEXT Fellow in the early part of this study. We are grateful to Emi Nishimoto and Hai-Ou Gu for technical assistance and Aki Miyazaki for administrative assistance.

AUTHOR CONTRIBUTIONS

H.L. designed and performed a large part of the experiments and analyzed data. T. Miki, N.W., C.H., and C.J.K. provided useful materials and advices. G.M.A. and T. Matsuzaki helped some part of the experiments. M.N. organized and supervised the study, designed and performed a part of the experiments, and analyzed data. H.L. and M.N. co-wrote the draft, which was improved by opinions and ideas provided by other authors.

DECLARATION OF INTERESTS

The authors declare no competing interests.

Received: February 19, 2019
Revised: May 28, 2019
Accepted: August 5, 2019
Published: September 27, 2019

REFERENCES

Almeida, G.M., Yamamoto, M., Morioka, Y., Ogawa, S., Matsuzaki, T., and Noda, M. (2015). Critical roles for murine Reck in the regulation of vascular patterning and stabilization. Sci. Rep. *5*, 17860.

Anderson, K.D., Pan, L., Yang, X.M., Hughes, V.C., Walls, J.R., Dominguez, M.G., Simmons, M.V., Burfeind, P., Xue, Y., Wei, Y., et al. (2011). Angiogenic sprouting into neural tissue requires Gpr124, an orphan G protein-coupled receptor. Proc. Natl. Acad. Sci. U S A *108*, 2807–2812.

Bader, B.L., Rayburn, H., Crowley, D., and Hynes, R.O. (1998). Extensive vasculogenesis, angiogenesis, and organogenesis precede lethality in mice lacking all alpha v integrins. Cell *95*, 507–519.

Briggs, L.E., Burns, T.A., Lockhart, M.M., Phelps, A.L., Van den Hoff, M.J., and Wessels, A. (2015). Wnt/beta-catenin and sonic hedgehog pathways interact in the regulation of the development of the dorsal mesenchymal protrusion. Dev. Dyn. *245*, 103–113.

Cambier, L., Plate, M., Sucov, H.M., and Pashmforoush, M. (2014). Nkx2-5 regulates cardiac growth through modulation of Wnt signaling by R-spondin3. Development *141*, 2959–2971.

Chandana, E.P., Maeda, Y., Ueda, A., Kiyonari, H., Oshima, N., Yamamoto, M., Kondo, S., Oh, J., Takahashi, R., Yoshida, Y., et al. (2010). Involvement of the Reck tumor suppressor protein in maternal and embryonic vascular remodeling in mice. BMC Dev. Biol. *10*, 84.

Cho, C., Smallwood, P.M., and Nathans, J. (2017). Reck and Gpr124 are essential receptor cofactors for Wnt7a/Wnt7b-specific signaling in mammalian CNS angiogenesis and blood-brain barrier regulation. Neuron *95*, 1221–1225.

Cohen, E.D., Wang, Z., Lepore, J.J., Lu, M.M., Taketo, M.M., Epstein, D.J., and Morrisey, E.E. (2007). Wnt/beta-catenin signaling promotes expansion of Isl-1-positive cardiac progenitor cells through regulation of FGF signaling. J. Clin. Invest. *117*, 1794–1804.

Cohen, E.D., Ihida-Stansbury, K., Lu, M.M., Panettieri, R.A., Jones, P.L., and Morrisey, E.E. (2009). Wnt signaling regulates smooth muscle precursor development in the mouse lung via a tenascin C/PDGFR pathway. J. Clin. Invest. *119*, 2538–2549.

Corada, M., Orsenigo, F., Morini, M.F., Pitulescu, M.E., Bhat, G., Nyqvist, D., Breviario, F., Conti, V., Briot, A., Iruela-Arispe, M.L., et al. (2013). Sox17 is indispensable for acquisition and maintenance of arterial identity. Nat. Commun. *4*, 2609.

Corada, M., Orsenigo, F., Bhat, G.P., Conze, L.L., Breviario, F., Cunha, S.I., Claesson-Welsh, L., Beznoussenko, G.V., Mironov, A.A., Bacigaluppi, M., et al. (2019). Fine-tuning of Sox17 and canonical Wnt coordinates the permeability properties of the blood-brain barrier. Circ. Res. *124*, 511–525.

Cornett, B., Snowball, J., Varisco, B.M., Lang, R., Whitsett, J., and Sinner, D. (2013). Wntless is required for peripheral lung differentiation and pulmonary vascular development. Dev. Biol. *379*, 38–52.

Cruciat, C.M., and Niehrs, C. (2012). Secreted and transmembrane wnt inhibitors and activators. Cold Spring Harb. Perspect. Biol. *5*, a015081.

Cullen, M., Elzarrad, M.K., Seaman, S., Zudaire, E., Stevens, J., Yang, M.Y., Li, X., Chaudhary, A., Xu, L., Hilton, M.B., et al. (2011). GPR124, an orphan G protein-coupled receptor, is required for CNS-specific vascularization and establishment of the blood-brain barrier. Proc. Natl. Acad. Sci. U S A *108*, 5759–5764.

Curtis, C.D., and Griffin, C.T. (2012). The chromatin-remodeling enzymes BRG1 and CHD4 antagonistically regulate vascular Wnt signaling. Mol. Cell. Biol. *32*, 1312–1320.

Da Silva, F., Rocha, A.S., Motamedi, F.J., Massa, F., Basboga, C., Morrison, H., Wagner, K.D., and Schedl, A. (2017). Coronary artery formation is driven by localized expression of R-spondin3. Cell Rep. *20*, 1745–1754.

Daneman, R., Agalliu, D., Zhou, L., Kuhnert, F., Kuo, C.J., and Barres, B.A. (2009). Wnt/beta-catenin signaling is required for CNS, but not non-CNS, angiogenesis. Proc. Natl. Acad. Sci. U S A *106*, 641–646.

Eubelen, M., Bostaille, N., Cabochette, P., Gauquier, A., Tebabi, P., Dumitru, A.C., Koehler, M., Gut, P., Alsteens, D., Stainier, D.Y.R., et al. (2018). A molecular mechanism for Wnt ligand-specific signaling. Science *361*, eaat1178.

Griffin, C.T., Curtis, C.D., Davis, R.B., Muthukumar, V., and Magnuson, T. (2011). The chromatin-remodeling enzyme BRG1 modulates vascular Wnt signaling at two levels. Proc. Natl. Acad. Sci. U S A *108*, 2282–2287.

Harada, N., Tamai, Y., Ishikawa, T., Sauer, B., Takaku, K., Oshima, M., and Taketo, M.M. (1999). Intestinal polyposis in mice with a dominant stable mutation of the beta-catenin gene. EMBO J. *18*, 5931–5942.

Hebert, J.M., and McConnell, S.K. (2000). Targeting of cre to the Foxg1 (BF-1) locus mediates loxP recombination in the telencephalon and other developing head structures. Dev. Biol. *222*, 296–306.

Hellbach, N., Weise, S.C., Vezzali, R., Wahane, S.D., Heidrich, S., Roidl, D., Pruszak, J., Esser, J.S., and Vogel, T. (2014). Neural deletion of Tgfbr2 impairs angiogenesis through an altered secretome. Hum. Mol. Genet. *23*, 6177–6190.

Hirabayashi, Y., Itoh, Y., Tabata, H., Nakajima, K., Akiyama, T., Masuyama, N., and Gotoh, Y. (2004). The Wnt/beta-catenin pathway directs neuronal differentiation of cortical neural precursor cells. Development *131*, 2791–2801.

Hirai, H., Matoba, K., Mihara, E., Arimori, T., and Takagi, J. (2019). Crystal structure of a mammalian Wnt-frizzled complex. Nat. Struct. Mol. Biol. *26*, 372–379.

Kisanuki, Y.Y., Hammer, R.E., Miyazaki, J., Williams, S.C., Richardson, J.A., and Yanagisawa, M. (2001). Tie2-Cre transgenic mice: a new model for endothelial cell-lineage analysis in vivo. Dev. Biol. *230*, 230–242.

Klein, P.S., and Melton, D.A. (1996). A molecular mechanism for the effect of lithium on development. Proc. Natl. Acad. Sci. U S A *93*, 8455–8459.

Kugimiya, F., Kawaguchi, H., Ohba, S., Kawamura, N., Hirata, M., Chikuda, H., Azuma, Y., Woodgett, J.R., Nakamura, K., and Chung, U.I. (2007). GSK-3beta controls osteogenesis through regulating Runx2 activity. PLoS One *2*, e837.

Kuhnert, F., Mancuso, M.R., Shamloo, A., Wang, H.T., Choksi, V., Florek, M., Su, H., Fruttiger, M., Young, W.L., Heilshorn, S.C., and Kuo, C.J. (2010). Essential regulation of CNS angiogenesis by the orphan G protein-coupled receptor GPR124. Science *330*, 985–989.

Liebner, S., Corada, M., Bangsow, T., Babbage, J., Taddei, A., Czupalla, C.J., Reis, M., Felici, A., Wolburg, H., Fruttiger, M., et al. (2008). Wnt/beta-catenin signaling controls development of the blood-brain barrier. J. Cell Biol. *183*, 409–417.

Lyden, D., Young, A.Z., Zagzag, D., Yan, W., Gerald, W., O'Reilly, R., Bader, B.L., Hynes, R.O., Zhuang, Y., Manova, K., and Benezra, R. (1999). Id1 and Id3 are required for neurogenesis, angiogenesis and vascularization of tumour xenografts. Nature *401*, 670–677.

Mazzoni, J., Smith, J.R., Shahriar, S., Cutforth, T., Ceja, B., and Agalliu, D. (2017). The Wnt inhibitor Apcdd1 coordinates vascular remodeling and barrier maturation of retinal blood vessels. Neuron *96*, 1055–1069.e6.

McCarty, J.H., Monahan-Earley, R.A., Brown, L.F., Keller, M., Gerhardt, H., Rubin, K., Shani, M., Dvorak, H.F., Wolburg, H., Bader, B.L., et al. (2002). Defective associations between blood vessels and brain parenchyma lead to cerebral hemorrhage in mice lacking alphav integrins. Mol. Cell. Biol. *22*, 7667–7677.

McCarty, J.H., Lacy-Hulbert, A., Charest, A., Bronson, R.T., Crowley, D., Housman, D., Savill, J., Roes, J., and Hynes, R.O. (2005). Selective ablation of alphav integrins in the central nervous system leads to cerebral hemorrhage, seizures, axonal degeneration and premature death. Development *132*, 165–176.

Morini, M.F., and Dejana, E. (2014). Transcriptional regulation of arterial differentiation via Wnt, Sox and Notch. Curr. Opin. Hematol. *21*, 229–234.

Muraguchi, T., Takegami, Y., Ohtsuka, T., Kitajima, S., Chandana, E.P., Omura, A., Miki, T., Takahashi, R., Matsumoto, N., Ludwig, A., et al. (2007). RECK modulates Notch signaling during cortical neurogenesis by regulating ADAM10 activity. Nat. Neurosci. *10*, 838–845.

Muzumdar, M.D., Tasic, B., Miyamichi, K., Li, L., and Luo, L. (2007). A global double-fluorescent Cre reporter mouse. Genesis *45*, 593–605.

Oh, J., Takahashi, R., Kondo, S., Mizoguchi, A., Adachi, E., Sasahara, R.M., Nishimura, S., Imamura, Y., Kitayama, H., Alexander, D.B., et al. (2001). The membrane-anchored MMP inhibitor

RECK is a key regulator of extracellular matrix integrity and angiogenesis. Cell *107*, 789–800.

Omura, A., Matsuzaki, T., Mio, K., Ogura, T., Yamamoto, M., Fujita, A., Okawa, K., Kitayama, H., Takahashi, C., Sato, C., and Noda, M. (2009). RECK forms cowbell-shaped dimers and inhibits matrix metalloproteinase-catalyzed cleavage of fibronectin. J. Biol. Chem. *284*, 3461–3469.

Paredes, I., Himmels, P., and Ruiz de Almodovar, C. (2018). Neurovascular communication during CNS development. Dev. Cell *45*, 10–32.

Privratsky, J.R., Newman, D.K., and Newman, P.J. (2010). PECAM-1: conflicts of interest in inflammation. Life Sci. *87*, 69–82.

Proctor, J.M., Zang, K., Wang, D., Wang, R., and Reichardt, L.F. (2005). Vascular development of the brain requires beta8 integrin expression in the neuroepithelium. J. Neurosci. *25*, 9940–9948.

Routledge, D., and Scholpp, S. (2019). Mechanisms of intercellular Wnt transport. Development *146*, https://doi.org/10.1242/dev.176073.

Shimomura, Y., Agalliu, D., Vonica, A., Luria, V., Wajid, M., Baumer, A., Belli, S., Petukhova, L., Schinzel, A., Brivanlou, A.H., et al. (2010). APCDD1 is a novel Wnt inhibitor mutated in hereditary hypotrichosis simplex. Nature *464*, 1043–1047.

Sinner, D., Kordich, J.J., Spence, J.R., Opoka, R., Rankin, S., Lin, S.C., Jonatan, D., Zorn, A.M., and Wells, J.M. (2007). Sox17 and Sox4 differentially regulate beta-catenin/T-cell factor activity and proliferation of colon carcinoma cells. Mol. Cell. Biol. *27*, 7802–7815.

Stenman, J.M., Rajagopal, J., Carroll, T.J., Ishibashi, M., McMahon, J., and McMahon, A.P. (2008). Canonical Wnt signaling regulates organ-specific assembly and differentiation of CNS vasculature. Science *322*, 1247–1250.

Sundberg, C., Nagy, J.A., Brown, L.F., Feng, D., Eckelhoefer, I.A., Manseau, E.J., Dvorak, A.M., and Dvorak, H.F. (2001). Glomeruloid microvascular proliferation follows adenoviral vascular permeability factor/vascular endothelial growth factor-164 gene delivery. Am. J. Pathol. *158*, 1145–1160.

Takahashi, C., Sheng, Z., Horan, T.P., Kitayama, H., Maki, M., Hitomi, K., Kitaura, Y., Takai, S., Sasahara, R.M., Horimoto, A., et al. (1998). Regulation of matrix metalloproteinase-9 and inhibition of tumor invasion by the membrane-anchored glycoprotein RECK. Proc. Natl. Acad. Sci. U S A *95*, 13221–13226.

Tian, Y., Yuan, L., Goss, A.M., Wang, T., Yang, J., Lepore, J.J., Zhou, D., Schwartz, R.J., Patel, V., Cohen, E.D., and Morrisey, E.E. (2010). Characterization and in vivo pharmacological rescue of a Wnt2-Gata6 pathway required for cardiac inflow tract development. Dev. Cell *18*, 275–287.

Ulrich, F., Carretero-Ortega, J., Menendez, J., Narvaez, C., Sun, B., Lancaster, E., Pershad, V., Trzaska, S., Veliz, E., Kamei, M., et al. (2016). Reck enables cerebrovascular development by promoting canonical Wnt signaling. Development *143*, 147–159.

Vallon, M., Yuki, K., Nguyen, T.D., Chang, J., Yuan, J., Siepe, D., Miao, Y., Essler, M., Noda, M., Garcia, K.C., and Kuo, C.J. (2018). A RECK-WNT7 receptor-ligand interaction enables isoform-specific regulation of Wnt bioavailability. Cell Rep. *25*, 339–349.e9.

Vanhollebeke, B., Stone, O.A., Bostaille, N., Cho, C., Zhou, Y., Maquet, E., Gauquier, A., Cabochette, P., Fukuhara, S., Mochizuki, N., et al. (2015). Tip cell-specific requirement for an atypical Gpr124- and Reck-dependent Wnt/beta-catenin pathway during brain angiogenesis. Elife *4*, e06489.

Yamamoto, M., Matsuzaki, T., Takahashi, R., Adachi, E., Maeda, Y., Yamaguchi, S., Kitayama, H., Echizenya, M., Morioka, Y., Alexander, D.B., et al. (2012). The transformation suppressor gene Reck is required for postaxial patterning in mouse forelimbs. Biol. Open *1*, 458–466.

Yang, D., Baumann, J.M., Sun, Y.Y., Tang, M., Dunn, R.S., Akeson, A.L., Kernie, S.G., Kallapur, S., Lindquist, D.M., Huang, E.J., et al. (2013). Overexpression of vascular endothelial growth factor in the germinal matrix induces neurovascular proteases and intraventricular hemorrhage. Sci. Transl. Med. *5*, 193ra190.

Zhu, J., Motejlek, K., Wang, D., Zang, K., Schmidt, A., and Reichardt, L.F. (2002). beta8 integrins are required for vascular morphogenesis in mouse embryos. Development *129*, 2891–2903.

Zorn, A.M., Barish, G.D., Williams, B.O., Lavender, P., Klymkowsky, M.W., and Varmus, H.E. (1999). Regulation of Wnt signaling by Sox proteins: XSox17 alpha/beta and XSox3 physically interact with beta-catenin. Mol. Cell *4*, 487–498.

ISCI, Volume *19*

Supplemental Information

RECK in Neural Precursor Cells Plays a Critical Role in Mouse Forebrain Angiogenesis

Huiping Li, Takao Miki, Glícia Maria de Almeida, Carina Hanashima, Tomoko Matsuzaki, Calvin J. Kuo, Naoki Watanabe, and Makoto Noda

Table S1. Primers for PCR, Related to Figures 1-5

Gene		5′-3′	Annealing temp. (℃)	Product size (bp)
Genotyping				
Cre	Forward	GCCTGCATTACCGGTCGATGCAAGG	65	700
	Reverse	AAATCCATCGCTCGAGTTTAGTTACCC		
Reck^{flex1}	Forward	TGGGCGGAAGGGATACGTAG	57→61	480
	Reverse	CACATCCGAACGCTGAGCAA		
qRT-PCR				
Mars	Forward	GAGGGTGTGTGTCCCTTCTG	59	202
	Reverse	CTGTCTTCCCCAACCAGTCC		
Gapdh	Forward	TCAACGGCACAGTCAAGG	59	126
	Reverse	ACTCCACGACATACTCAGC		
Reck	Forward	AGGTCTCCAGCAGTCTTC	59	137
	Reverse	GCAGTTCCTTCCAGTTGTG		
Mmp2	Forward	CAAGTTCCCCGGCGATGTC	59	171
	Reverse	TTCTGGTCAAGGTCACCTGTC		
Wnt7a	Forward	GGCTTCTCTTCGGTGGTAGC	59	155
	Reverse	TGAAACTGACACTCGTCCAGG		
Wnt7b	Forward	TTTGGCGTCCTCTACGTGAAG	59	145
	Reverse	CCCCGATCACAATGATGGCA		
Itgb8	Forward	AGTGAACACAATAGATGTGGCTC	59	115
	Reverse	TTCCTGATCCACCTGAAACAAAA		
Itgb1	Forward	ATGCCAAATCTTGCGGAGAAT	59	209
	Reverse	TTTGCTGCGATTGGTGACATT		
Glut1	Forward	CAGTTCGGCTATAACACTGGTG	59	156
	Reverse	GCCCCCGACAGAGAAGATG		
Vegfa	Forward	GCACATAGAGAGAATGAGCTTCC	59	105
	Reverse	CTCCGCTCTGAACAAGGCT		
Nes	Forward	CCCTGAAGTCGAGGAGCTG	59	166
	Reverse	CTGCTGCACCTCTAAGCGA		
Tubb3	Forward	TAGACCCCAGCGGCAACTAT	59	127
	Reverse	GTTCCAGGTTCCAAGTCCACC		
Id1	Forward	CCTAGCTGTTCGCTGAAGGC	59	60
	Reverse	CTCCGACAGACCAAGTACCAC		
Id3	Forward	CTGTCGGAACGTAGCCTGG	59	90
	Reverse	GTGGTTCATGTCGTCCAAGAG		
Axin2	Forward	TGACTCTCCTTCCAGATCCCA	59	105
	Reverse	TGCCCACACTAGGCTGACA		
Apcdd1	Forward	ATGAACACCACCCTCCCATAC	59	161
	Reverse	GTAGTAATGCCCTTCCCAGGT		
Sox17	Forward	GATGCGGGATACGCCAGTG	59	136
	Reverse	CCACCACCTCGCCTTTCAC		

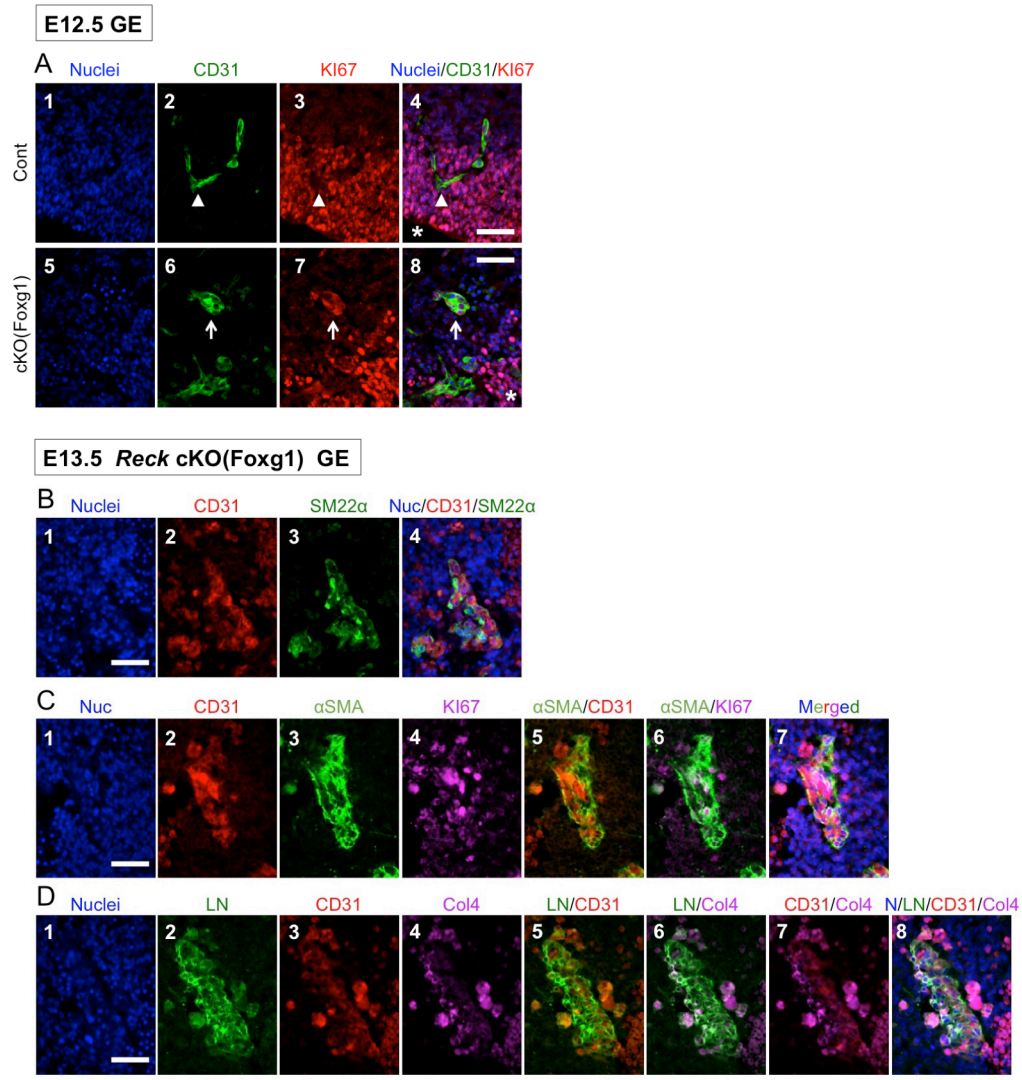

Figure S1. Characterization of abnormal vessels, Related to Figures 2 and 3.

(A) Proliferating cells as detected by Ki67-immunofluorescence staining. Coronal sections of the brain from control (panels 1-4) and Reck-cKO (Foxg1) mice (panels 5-8) at E12.5 were doubly stained with anti-CD31 (endothelial marker, green; panels 2 and 6) and anti-Ki67 (proliferation marker, red; panels 3 and 7) antibodies followed by nuclear counterstaining (blue; panels 1 and 5). Merged images of the red, green, and blue fluorescence are also included (panels 4 and 8). Typical images focusing on vessels in ganglionic eminence are shown. Asterisk indicates the ventricular side. Note that CD31-positive vascular endothelial cells are largely Ki67-negative in control mice (arrowheads in panels 3 and 4) while clusters of CD31-positive cells found in Reck-cKO (Foxg1) mice

are often Ki67-positive (arrow in panels 7 and 8), indicating proliferative nature of these cells.
(B, C) Distribution of mesenchymal antigens in vascular malformations found in Reck-cKO (Foxg1) mice. Coronal sections of the brain from Reck-cKO (Foxg1) mice at E13.5 were stained for endothelial marker (CD31, red; panel 2) and mesenchymal marker [SM22a (B, panel 3) or α-smooth muscle actin (αSMA; C, panel 3)], without (B) or with Ki67 (C, magenta, panel 4), followed by nuclear counterstaining (blue; panel 1). Note that the endothelial and mesenchymal signals are largely non-overlapped in vascular malformations in merged images (B4 and C5), which does not support the involvement of endothelial-to-mesenchymal transition (EndMT) (Dejana and Lampugnani, 2018). Ki67-signals are associated with many CD31-positive cells (C6 and C7), again indicating the proliferative nature of these endothelial cell clusters.
(D) Distribution of basement membrane markers around the abnormal vessels found in Reck-cKO (Foxg1) mice. The brain sections were stained for endothelial marker (CD31, red; panel 3) and two basement membrane markers, laminin (LN, green; panel 2) and type IV collagen (Col4, magenta; panel 4). Scale bar: 50 μm.

[1] E11.5

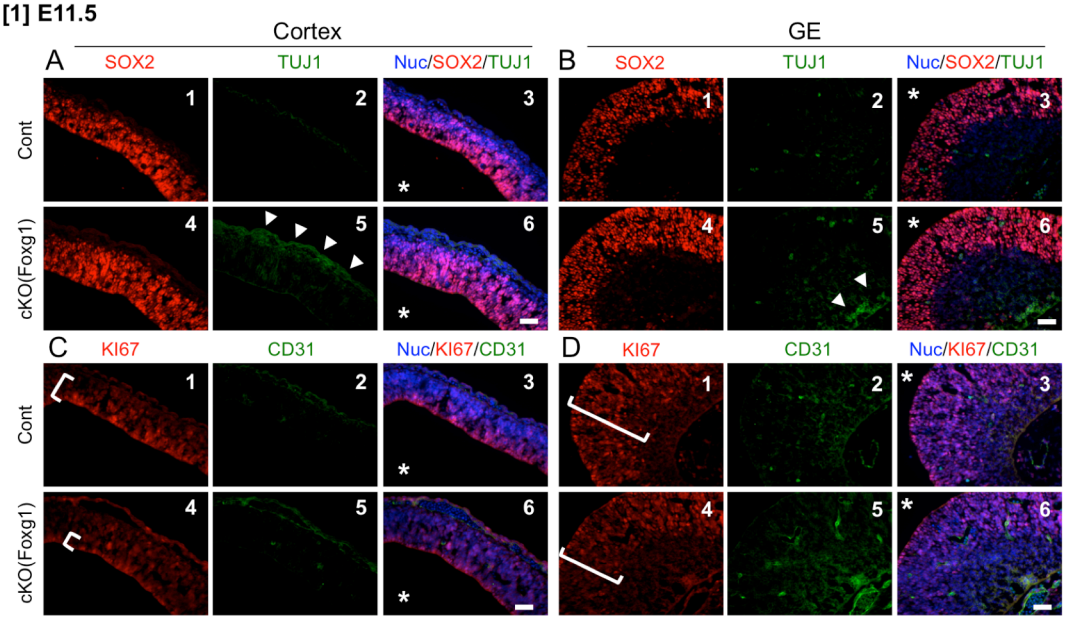

[2] E12.5

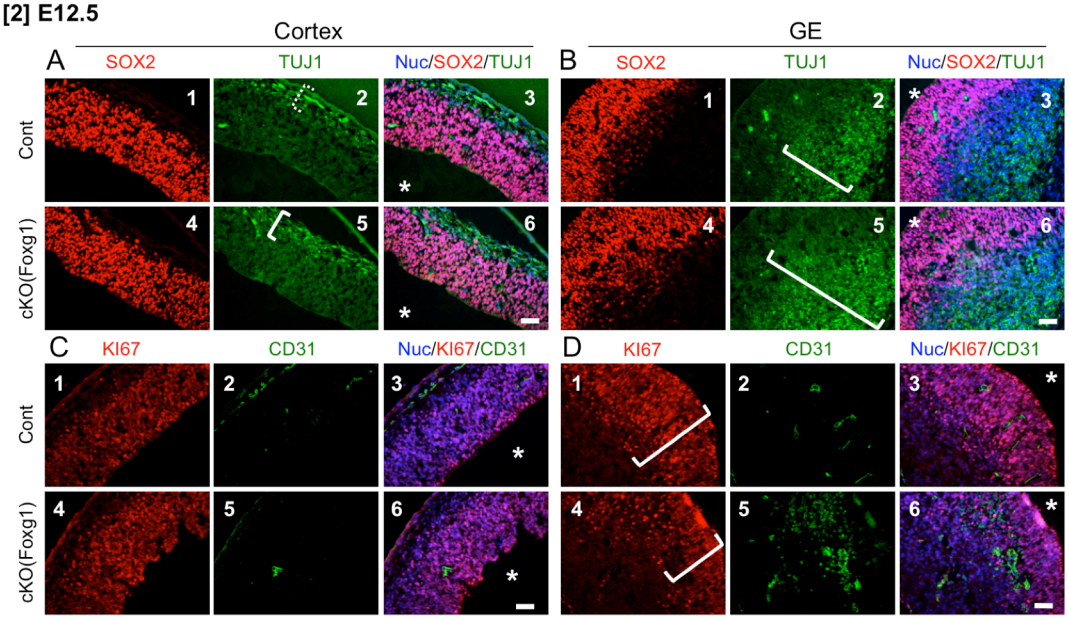

[3] E13.5

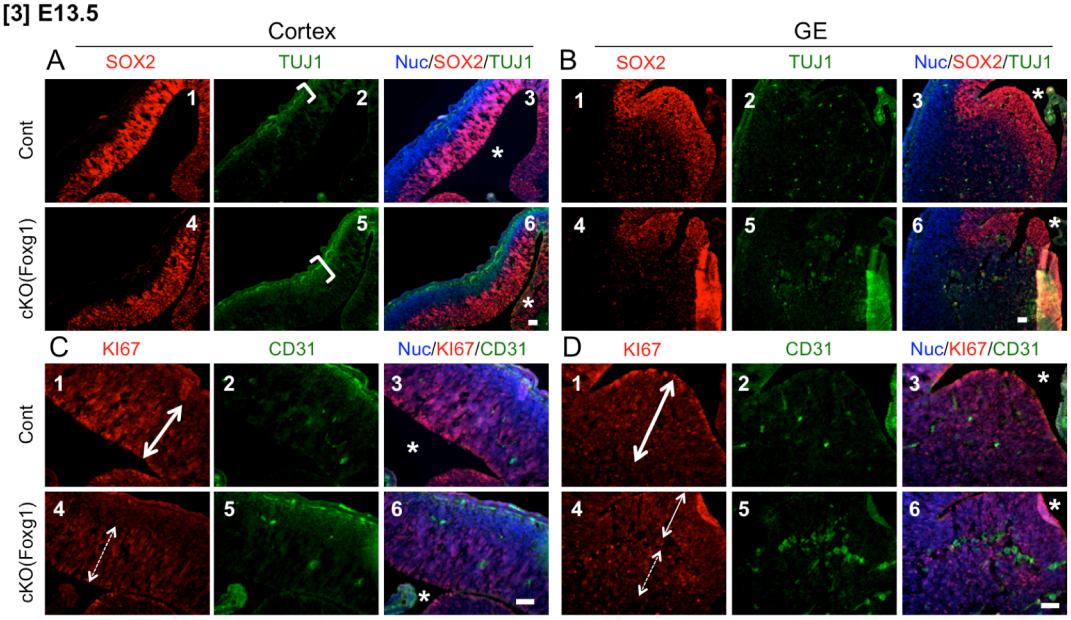

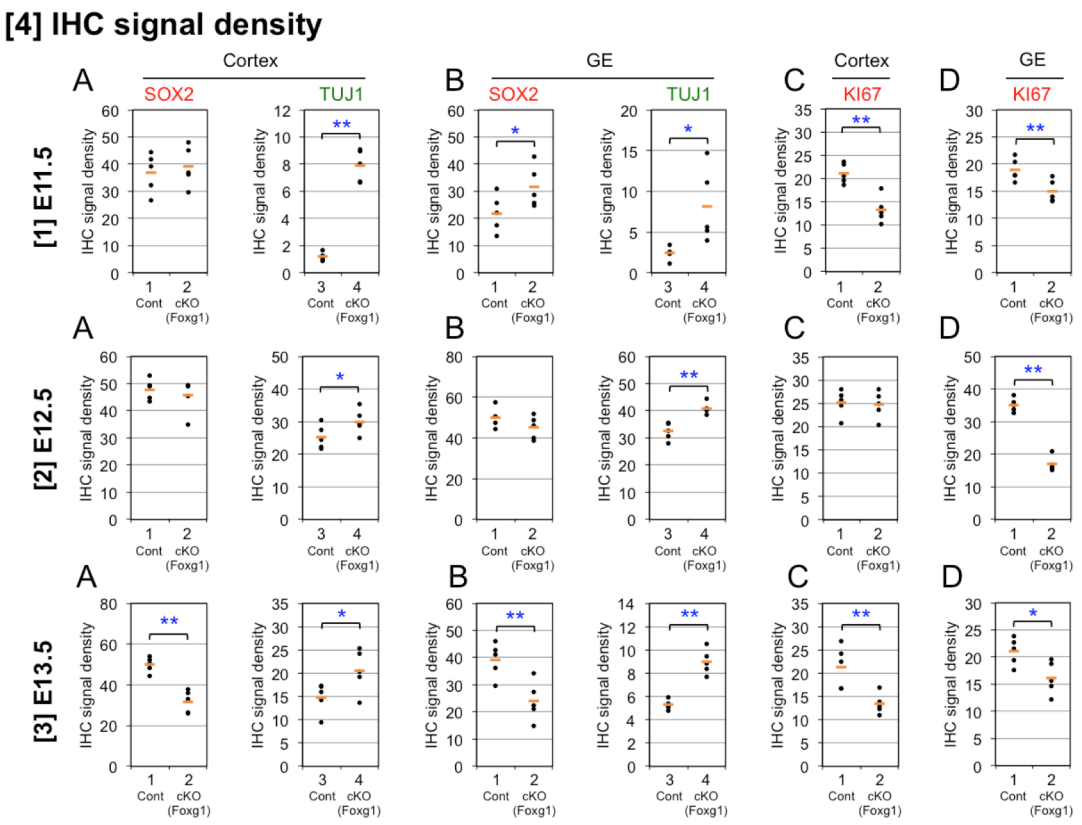

Figure S2. Neural phenotype of Reck-cKO (Foxg1) mouse at three embryonic stages, Related to Figure 2q.

Coronal sections of the brain from a control (panels 1-3) or a Reck-cKO (Foxg1) mouse (panels 4-6) at E11.5 (set [1]), E12.5 (set [2]), or E13.5 (set [3]) were doubly stained with anti-Sox2 (neural precursor marker, red; A, B, panels 1, 4) and anti-TUJ1 (neuronal marker, green; A, B, panels 2, 5) antibodies or with anti-Ki67 (proliferation marker, red; C, D, panels 1, 4) and anti-CD31 (endothelial marker, green; C, D, panels 2, 5) antibodies followed by nuclear counterstain (blue). Merged images of the red, green, and blue fluorescence are also included (panels 3 and 6). Typical images focusing on the cerebral cortex (A, C) or ganglionic eminence (B, D) are shown. Symbols in [1]-[3]: asterisk, ventricle; arrowhead, signals of interest; bracket and double-pointed arrow, layer of positive cells, with some semi-quantitative information such as thickness of the layer (length), intensity (line thickness), and sparseness (dotted line). Scale bar: 50 μm. The images in set [3] A and B are at a lower magnification (x10 objective lens) than others (x20 objective lense). [4] Fluorescence density per unit area in

images as shown in [1]-[3] was determined using ImageJ (see Methods for detail). Dot represents the density in one area, and brown horizontal bar the mean of 5 areas. Significance of difference is indicated by asterisk(s): * $P<0.05$, ** $P<0.01$. Note that in Reck-cKO (Foxg1) mice, TUJ1-positive mature neurons tend to be more abundant and widely distributed while Ki67-positive cells are less abundant than the control at all three stages. At E13.5, decreased abundance of Sox2-positive cells becomes also apparent (bottom row, group 2 in A and B).

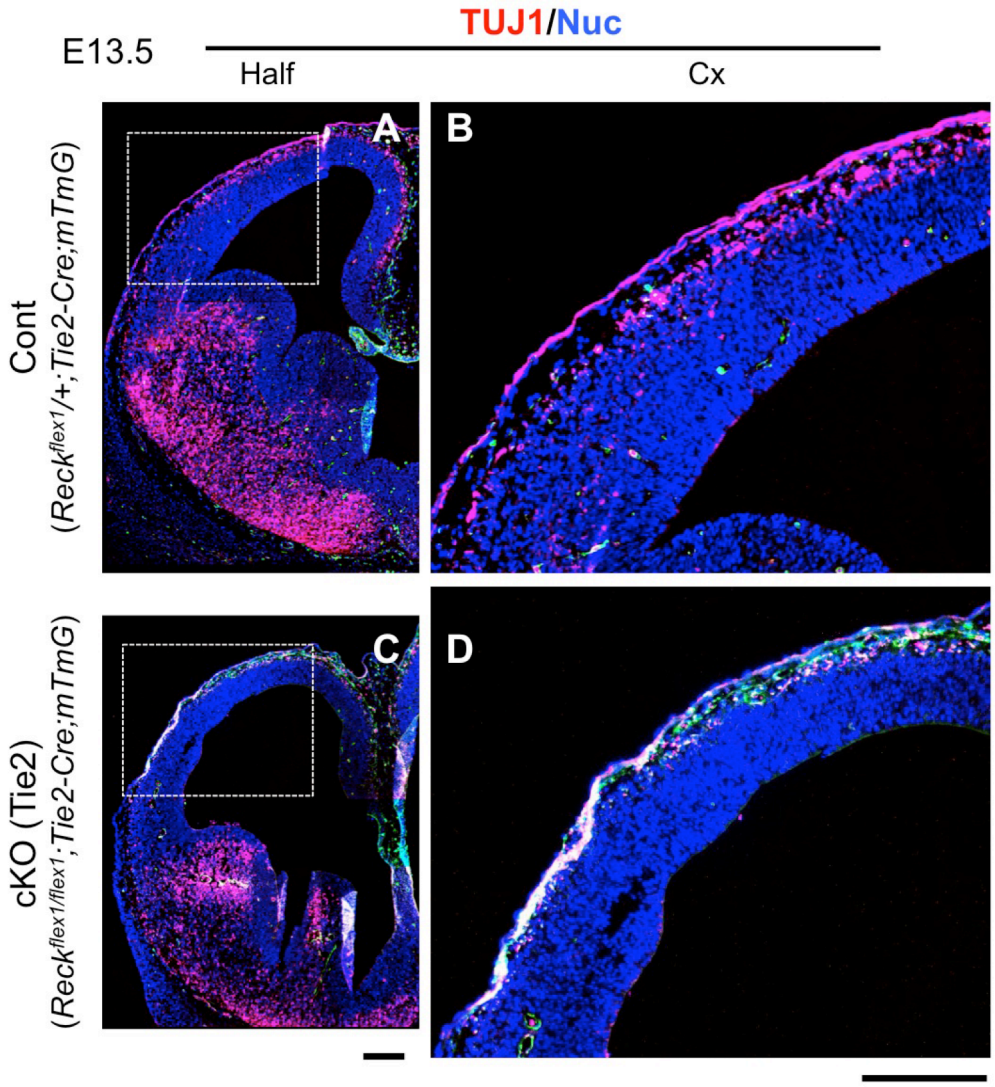

Figure S3. Neural phenotype of Reck-cKO (Tie2) mouse at E13.5, Related to Figures 2q and Figure 3I-P.

A coronal section of the brain from control (A, B) or Reck-cKO (Tie2) mouse (C, D) at E13.5 were stained with anti-TUJ1 antibodies (neuronal marker, red) followed by nuclear counterstain (blue). Magnified views of the cortical area (dotted-line box) in panels A and C are shown in B and D, respectively. Note the less prominent TUJ1 signals (red) in the Reck-cKO (Tie2) mouse brain (panels C, D) than the control (panels A, B). Scale bars: 200 μm.

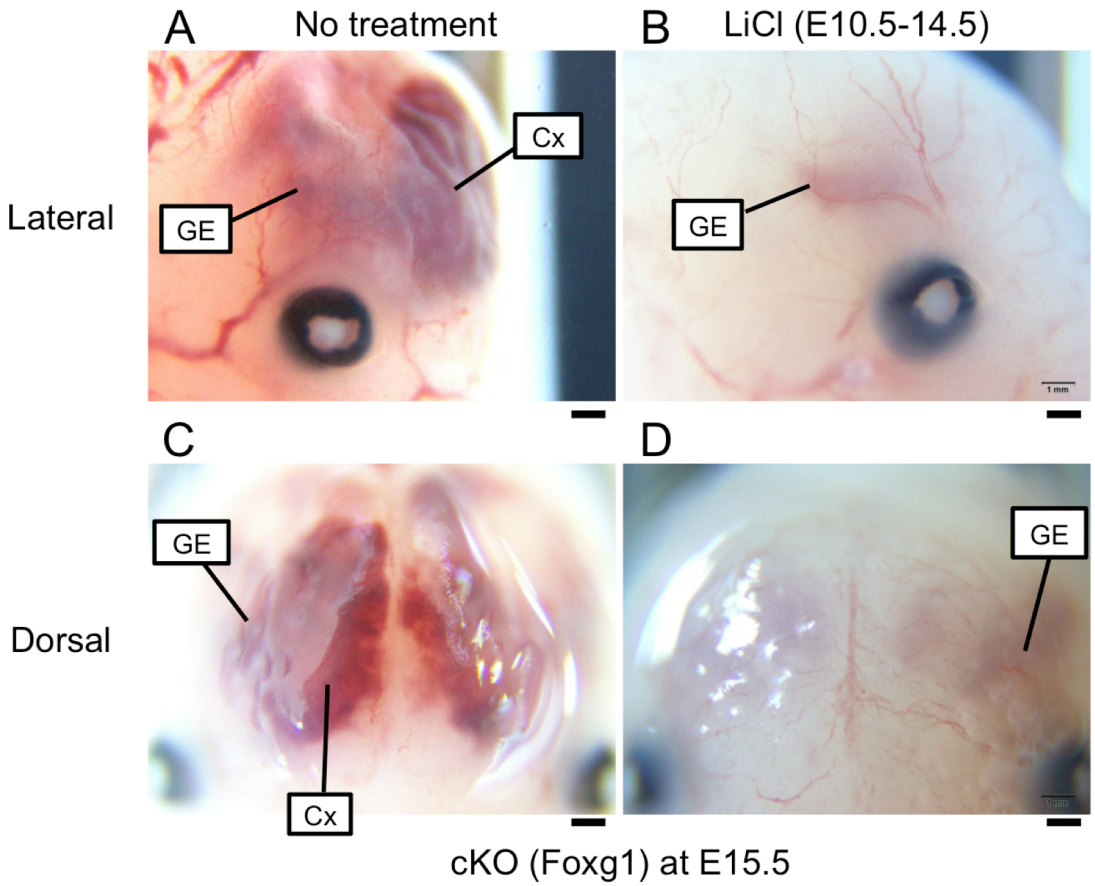

Figure S4. Vascular phenotype of Reck-cKO (Foxg1) mice at E15.5 after LiCl-treatment, Related to Table 1 and Figure 4. Lateral (A, B) and dorsal (C, D) views, focusing on the head region, of Reck-cKO (Foxg1) embryos left untreated (A, C) or treated with LiCl daily from E10.5 to E14.5 (B, D) and harvested at E15.5. GE, hemorrhage in ganglionic eminence. Cx, hemorrhage in cerebral cortex. Scale bar: 1 mm.

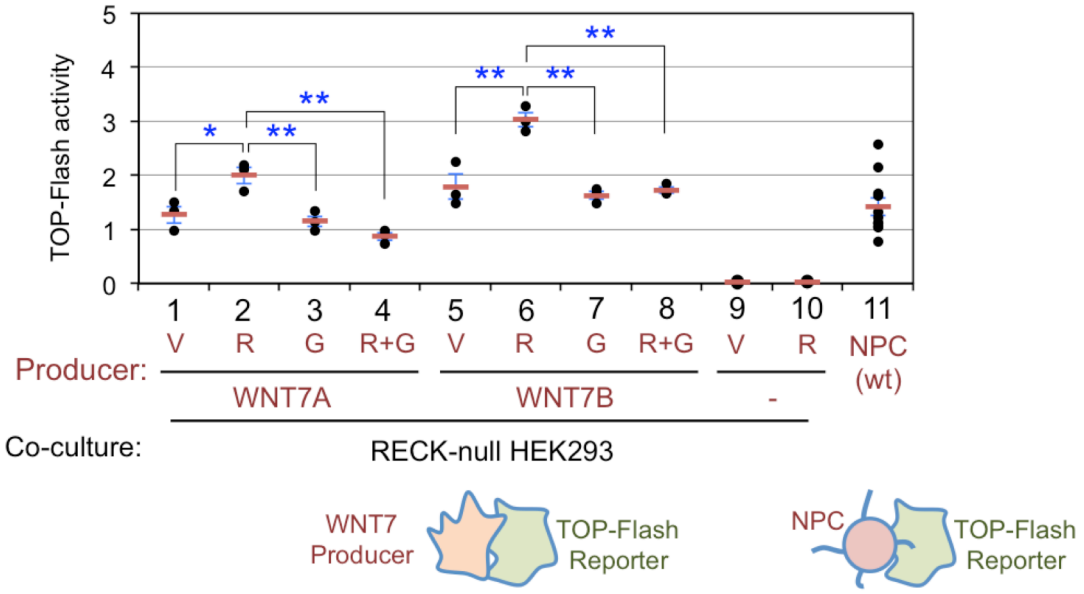

Figure S5. Effects of RECK and GPR124 in WNT7-producing HEK293 cells on WNT signaling in the reporter cells in mixed culture, Related to Figure 5, D and E.

RECK-deficient HEK293 cells stably expressing WNT7A (groups 1-4) or WNT7B (groups 5-8) were transfected with either control vector (V), RECK-expression vector (R), GPR124-expression vector (G), or both expression vectors (R+G), incubated for 48 h, and then co-cultured for 24 h with TOP-Flash reporter cells lacking RECK, followed by dual-luciferase assay (in triplicate). The cells without WNT7-expression (groups 9, 10) and wild type NPCs (group 11) were also included for comparison. *P<0.05, **P<0.01. Note that GPR124 suppressed, rather than enhanced, the activity of RECK to enhance WNT signaling in adjacent reporter cells. Experiments were repeated three times with similar results.

TRANSPARENT METHODS

Mice

All animal experiments were approved by the Animal Research Committee, Graduate School of Medicine, Kyoto University and conducted according to its regulation. The engineered *Reck* allele *Reck*^{flex1}, carrying two lox-P sites franking the exon 1 ("flex1" stands for "floxed at exon 1"; tm2.1Noda, RRID:IMSR_RBRC10232), has been reported (Yamamoto et al., 2012). To generate Reck-cKO (Foxg1) mice, *Reck*$^{flex1/flex1}$ mice were crossed with mice carrying the *Foxg1-Cre* allele (Hebert and McConnell, 2000) to obtain the heterozygous *Reck*$^{flex1/+}$*; Foxg1-Cre* mice. These mice were crossed again with *Reck*$^{flex1/flex1}$ mice to obtain *Reck*$^{flex1/flex1}$*;Foxg1-Cre* [Reck-cKO (Foxg1)] and *Reck*$^{flex1/+}$*;Foxg1-Cre* [Cont] mice among others. To generate the EC-selective *Reck* knockout mice [Reck-cKO (Tie2)], *Reck*$^{flex1/flex1}$ mice were crossed with *Tie2-Cre* mice (Kisanuki et al., 2001) to obtain the heterozygous *Reck*$^{flex1/+}$*;Tie2-Cre* mice. These mice were crossed again with *Reck*$^{flex1/flex1}$ mice to obtain *Reck*$^{flex1/flex1}$*;Tie2-Cre* [Reck-cKO (Tie2)] and *Reck*$^{flex1/+}$*;Tie2-Cre* [Cont] mice among others. To visualize Foxg1-Cre-expressed cells, the *Foxg1-Cre* mice were crossed with homozygous *mTmG/mTmG* mice (Muzumdar et al., 2007). Mice were mated between 16:00 and 9:00, and the day on which vaginal plug was found was designated as 0.5 dpc (E0.5). Genotype was determined by PCR using the primers listed in Supplemental Table S1.

Histology

Mouse embryos at indicated time points were harvested on ice, and the forebrain were harvested and fixed in 4% PFA solution overnight. After immersed in 10%/20%/30% sucrose/PBS solution, the forebrains were embedded in OCT and frozen. For Hematoxylin and Eosin (HE) staining, 10-μm thick cryosections were used. For immunofluorescence staining, 5-μm thick cryosections were incubated with primary antibodies overnight, washed, incubate with appropriate secondary antibodies (conjugated with either Alexa Fluor-488, -555, or -647) for 2 h at room temperature, and then washed and mounted using DAPI Fluoromount-G (0100-20, Southern Biotechnology Associates). Micrographs were acquired using Zeiss AxioPlan or Keyence

BZ-9000. Primary antibodies used: rat monoclonal anti-PECAM/CD31 (BD Bioscience, 553370), rabbit polyclonal anti-NG2 (Merck Millipore, AB5320), Mouse monoclonal anti-Laminin(clone LAM-89) (Sigma-Aldrich, L8271), Rabbit polyclonal anti-Type IV Collagen (PROGEN Biotechnik,10760), Goat polyclonal anti-Sox2 (Santa Cruz Biotechnology, sc-17320), Rabbit polyclonal anti-Neuronal Class III beta-Tubulin/TUJ1 (COVANCE, PRB-435P),and Rabbit polyclonal anti-Ki67 (Leica Biosystems, NCL-Ki67p). Secondary antibodies used: Goat anti-rat IgG(H+L) highly cross-adsorbed secondary antibodies (Alexa-555, Alexa-594, or Alexa-647 conjugates), and goat anti-rabbit IgG(H+L) highly cross-adsorbed secondary antibodies (Alexa-488 or Alexa-647 conjugates), Donkey anti-goat IgG(H+L) cross-adsorbed secondary antibodies (Alexa-647conjugates), Donkey anti-rabbit IgG(H+L) cross-adsorbed secondary antibodies (Alexa-488 conjugates) (Thermo Fisher Scientific). For densitometry, mean density of fluorescence signals per pixel in a scare ROI (90 x 90 pixels) was determined using ImageJ. Five ROIs were randomly selected in the region adjacent to the ventricle (in the cases of Sox2 and Ki67) or outer surface of the brain (in the case of TuJ1) in microscopic images acquired under comparable conditions.

Lithium Chloride Treatment

Reck^{flex1}*/+;Foxg1-Cre* male mice and *Reck*$^{flex1/flex1}$ female mice were timed-mated, and aqueous LiCl solution was injected (200 mg/kg, i.p.) into the female mice on several consecutive days as described in Table 1. Embryos were harvested at E15.5, and their cerebral hemorrhage was visually inspected (see Supplemental Figure S4), while their genotypes determined using yolk sac DNA.

qRT-PCR

Total RNA was extracted from forebrains of embryos at E11.5, E12.5, and E13.5 using Nucleo Spin RNA kit (Macherey-Nagel). cDNA was prepared using PrimeScript II 1st Strand cDNA synthesis kit (Takara), and quantitative PCR was performed with the Stratagene Mx3005P (Agilent) using KAPA SYBR Fast Universal qPCR kit (Kapa Biosystems) and the primers listed in Supplemental

Table S1. Ratio of mRNA in Reck-cKO (Foxg1) and Cont samples was calculated using the delta delta Ct method.

NPCs

NPCs were prepared according to the method of Kitani et al. (Kitani et al., 1991). Briefly, the forebrains of E11.5 embryos were cut into several pieces in DME/F12 medium. Eye cups, nasal plates, and other non neuroepithelial tissues were removed under a dissection microscope. The tissue pieces were treated with PBS containing 0.5% trypsin for 1 h at 37°C and then with DNase I to reduce viscosity. The cells were transferred to DME/F12 medium supplemented with 10% FBS on 12 well plates. After incubation for 7 h at 37°C in a CO_2 incubator, cells in the NPC-enriched fraction (floating cells) were collected, counted, and sedimented by centrifugation. The cells and the supernatant were separated and used in TOP-Flash assays.

TOP-Flash Assay

A *RECK*-deficient HEK293 sub-line, ADA99-25 (Matsuzaki et al. unpublished), was generated using the CRISPR/Cas9 double nickase method (Ran et al., 2013). To establish the RECK-deficient TOP-Flash reporter, ADA99-25 cells were transfected with pGL4.49 (Clontech) using CalPhos Mammalian Transfection Kit (Clontech), selected in growth medium (DMEM supplemented with 10% fetal bovine serum and Pen Strep) containing 100 μg/ml Hygromycin B Gold (Invitrogen), and a clone (named HNM1) whose firefly luciferase activity shows robust response to 20 μM LiCl was selected. To establish a WNT7-selective TOP-Flash reporter (named LC20b), HNM1 cells were co-transfected with four expression vectors (expressing Fzd4, Lrp5, GPR124, and RECK) (Takahashi et al., 1998; Vallon et al., 2018) and two marker plasmids [pRL (Promega) and pUCSV-BSD (Kimura et al., 1994)], selected in growth medium containing 8 μg/ml Blasticidin-S, and a clone was isolated whose firefly luciferase activity showed a robust response when co-cultured with HEK293 cells producing WNT7A. For TOP-Flash assay with NPCs, LC20b cells (3×10^4/well) were plated onto a white 96-well plate (BD 353296) at day 0. NPCs (3×10^4/well) or their culture supernatant were overlaid at day 1, and luciferase

assay was performed at day 2 using Dual-Glo Luciferase Assay System (Promega) or twinlite Firefly & Renilla Luciferase Reporter Gene Assay System (PerkinElmer). For TOP-Flash assay with HEK293 cells, we first established RECK-deficient HEK293 cells expressing either WNT7A or WNT7B by stably transfecting ADA99-25 cells with an expression vector (carrying the *neo* marker) expressing WNT7A or WNT7B (Vallon et al., 2018) followed by selection in growth medium containing 1 mg/ml G418. These WNT7 producer cells were transfected with either vacant vector (V) or RECK-expression vector (R) using FuGENE HD (Promega) and plated onto a white 96-well plate (1.5×10^4/well) at day 0 (Producer). In parallel, HNM1 cells were co-transfected with five expression vectors (pRL, Fzd4, Lrp5, GPR124, plus control or RECK-expressing vector) using FuGENE HD and plated onto regular dishes (Reporter). At day 1, media in all cultures were replaced to fresh growth medium. At day 2, culture supernatant on white plate (Producer) were transferred to new wells (Conditioned media), and then the Reporter cells, suspended using trypsin and washed with growth medium, were plated (3×10^4/well) onto the wells containing either the Producer cells or the Conditioned media. After 1-day incubation, luciferase assay was performed using the twinlite system.

Statistics

Quantitative data are presented in the form of dot plots with either open bar (Figure 5A) or horizontal lines (brown and blue) representing mean and the standard error of mean (s.e.m.) (Figure 5B-E). Significance of difference between two groups was assessed using Student's t-test.

Supplemental References

Dejana, E., and Lampugnani, M.G. (2018). Endothelial cell transitions. Science *362*, 746-747.

Hebert, J.M., and McConnell, S.K. (2000). Targeting of cre to the Foxg1 (BF-1) locus mediates loxP recombination in the telencephalon and other developing head structures. Dev Biol *222*, 296-306.

Kimura, M., Takatsuki, A., and Yamaguchi, I. (1994). Blasticidin S deaminase gene from Aspergillus terreus (BSD): a new drug resistance gene for transfection of mammalian cells. Biochim Biophys Acta *1219*, 653-659.

Kisanuki, Y.Y., Hammer, R.E., Miyazaki, J., Williams, S.C., Richardson, J.A., and Yanagisawa, M. (2001). Tie2-Cre transgenic mice: a new model for endothelial cell-lineage analysis in vivo. Dev Biol *230*, 230-242.

Kitani, H., Shiurba, R., Sakakura, T., and Tomooka, Y. (1991). Isolation and characterization of mouse neural precursor cells in primary culture. In Vitro Cell Dev Biol *27A*, 615-624.

Muzumdar, M.D., Tasic, B., Miyamichi, K., Li, L., and Luo, L. (2007). A global double-fluorescent Cre reporter mouse. Genesis *45*, 593-605.

Ran, F.A., Hsu, P.D., Wright, J., Agarwala, V., Scott, D.A., and Zhang, F. (2013). Genome engineering using the CRISPR-Cas9 system. Nat Protoc *8*, 2281-2308.

Takahashi, C., Sheng, Z., Horan, T.P., Kitayama, H., Maki, M., Hitomi, K., Kitaura, Y., Takai, S., Sasahara, R.M., Horimoto, A., Ikawa, Y., Ratzkin, B.J., Arakawa, T., and Noda, M. (1998). Regulation of matrix metalloproteinase-9 and inhibition of tumor invasion by the membrane-anchored glycoprotein RECK. Proc Natl Acad Sci U S A *95*, 13221-13226.

Vallon, M., Yuki, K., Nguyen, T.D., Chang, J., Yuan, J., Siepe, D., Miao, Y.,

Essler, M., Noda, M., Garcia, K.C., and Kuo, C.J. (2018). A RECK-WNT7 Receptor-Ligand Interaction Enables Isoform-Specific Regulation of Wnt Bioavailability. Cell Rep *25*, 339-349 e339.

Yamamoto, M., Matsuzaki, T., Takahashi, R., Adachi, E., Maeda, Y., Yamaguchi, S., Kitayama, H., Echizenya, M., Morioka, Y., Alexander, D.B., Yagi, T., Itohara, S., Nakamura, T., Akiyama, H., and Noda, M. (2012). The transformation suppressor gene Reck is required for postaxial patterning in mouse forelimbs. Biol Open *1*, 458-466.